Recursive marginal quantization of the Euler scheme of a diffusion process

Gilles Pagès, Abass Sagna

Recursive marginal quantization of the Euler scheme of a diffusion process

GILLES PAGÈS [*]   ABASS SAGNA [†] [‡]

Abstract

We propose a new approach to quantize the marginals of the discrete Euler diffusion process. The method is built recursively and involves the conditional distribution of the marginals of the discrete Euler process. Analytically, the method raises several questions like the analysis of the induced quadratic quantization error between the marginals of the Euler process and the proposed quantizations. We show in particular that at every discretization step t_k of the Euler scheme, this error is bounded by the cumulative quantization errors induced by the Euler operator, from times $t_0 = 0$ to time t_k. For numerics, we restrict our analysis to the one dimensional setting and show how to compute the optimal grids using a Newton-Raphson algorithm. We then propose a closed formula for the companion weights and the transition probabilities associated to the proposed quantizations. This allows us to quantize in particular diffusion processes in local volatility models by reducing dramatically the computational complexity of the search of optimal quantizers while increasing their computational precision with respect to the algorithms commonly proposed in this framework. Numerical tests are carried out for the Brownian motion and for the pricing of European options in a local volatility model. A comparison with the Monte Carlo simulations shows that the proposed method may sometimes be more efficient (w.r.t. both computational precision and time complexity) than the Monte Carlo method.

1   Introduction

Optimal quantization method appears first in [25] where the author studies in particular the optimal quantization problem for the uniform distribution. It has become an important field of information theory since the early 1940's. A common use of quantization is the conversion of a continuous signal into a discrete signal that assumes only a finite number of values.

Since then, optimal quantization has been applied in many fields like in Signal Processing, in Data Analysis, in Computer Sciences and recently in Numerical Probability following the work [14]. Its application to Numerical Probability relies on the possibility to discretize a random vector X taking infinitely many values by a discrete random vector $\hat{X}$ valued in a set of finite cardinality. This allows to approximate either expectations of the form $\mathbb{E}f(X)$ or, more significantly, some conditional expectations like $\mathbb{E}(f(X)|Y)$ (by quantizing both random variables X and Y). Optimal quantization is used to solve problems emerging in Quantitative Finance as optimal stopping problems (see [1, 2]), the pricing

---

[*]Laboratoire de Probabilités et Modèles aléatoires (LPMA), UPMC-Sorbonne Université, UMR CNRS 7599, case 188, 4, pl. Jussieu, F-75252 Paris Cedex 5, France. E-mail: `gilles.pages@upmc.fr`

[†]ENSIIE & Laboratoire de Mathématiques et Modélisation d'Evry (LaMME), Université d'Evry Val-d'Essonne, UMR CNRS 8071, 23 Boulevard de France, 91037 Evry. E-mail: `abass.sagna@ensiie.fr`.

of swing options (see [4]), stochastic control problems (see [7, 16]), nonlinear filtering problems (see e.g. [15, 22, 6, 23]), the pricing of barrier options (see [24]).

In Quantitative Finance, several problems of interest amount to estimate quantities of the form

$$\mathbb{E}\big[f(X_T)\big], \quad T > 0, \tag{1}$$

for a given Borel function $f : \mathbb{R}^d \to \mathbb{R}$, or involving terms like

$$\mathbb{E}\big[f(X_t)|X_s = x\big], \quad 0 < s < t, \tag{2}$$

where $(X_t)_{t\in[0,T]}$ is a stochastic diffusion process, solution to the stochastic differential equation

$$X_t = X_0 + \int_0^t b(s, X_s)ds + \int_0^t \sigma(s, X_s)dW_s, \tag{3}$$

where W is a standard q-dimensional Brownian motion starting at 0 independent of the $\mathbb{R}^d$-valued random vector X_0, both defined on a probability space $(\Omega, \mathcal{A}, \mathbb{P})$. The functions $b : [0, T] \times \mathbb{R}^d \to \mathbb{R}^d$ and the matrix-valued diffusion coefficient function $\sigma : [0, T] \times \mathbb{R}^d \to \mathbb{R}^{d\times q}$ are Borel measurable and satisfy some appropriate Lipschitz continuity and linear growth conditions to ensure the existence of a strong solution of the stochastic differential equation (see (21) and (20) further on). Since in general the solution of (3) is not explicit, we have first to approximate the continuous paths of the process $(X_t)_{t\in[0,T]}$ by a discretization scheme, typically, the Euler scheme. Given the (regular) time discretization mesh $t_k = k\Delta, k = 0, \ldots, n, \Delta = T/n$, the "discrete time Euler scheme" $(\bar{X}_{t_k}^n)_{k=0,\ldots,n}$, associated to $(X_t)_{t\in[0,T]}$ is recursively defined by

$$\bar{X}_{t_{k+1}}^n = \bar{X}_{t_k}^n + b(t_k, \bar{X}_{t_k}^n)\Delta + \sigma(t_k, \bar{X}_{t_k}^n)(W_{t_{k+1}} - W_{t_k}), \quad \bar{X}_0^n = X_0.$$

Then, once we have access to the discretization scheme of the stochastic process $(X_t)_{t\in[0,T]}$, the quantities (1) and (2) can be estimated by
$$\mathbb{E}\big[f(\bar{X}_T^n)\big] \tag{4}$$

and
$$\mathbb{E}\big[f(\bar{X}_{t_{k+1}}^n)|\bar{X}_{t_k}^n = x\big] \quad \text{when } t = t_{k+1} \text{ and } s = t_k. \tag{5}$$

Remark 1.1. (a) Note that, if b and σ both have linear growth in x uniformly in $t \in [0, T]$, then any strong solution to (3) (if any) and the Euler scheme satisfy for every $p \in (0, +\infty)$,

$$\sup_{n\geq 1} \mathbb{E}\Big(\max_{k=0,\ldots,n} |\bar{X}_{t_k}^n|^p \Big) + \mathbb{E}\Big(\sup_{t\in[0,T]} |X_t|^p \Big) < +\infty. \tag{6}$$

Hence, the above quantities (1), (2), (4), (5), are well defined as soon as f has polynomial growth (when X is well defined).

(b) When b and σ are smooth with bounded derivatives, say C_b^4, the following weak error result holds for smooth functions f with polynomial growth (or bounded Borel functions under hypo-ellipticity assumptions on σ, see e.g. [3, 26]), the estimation of $\mathbb{E}\big[f(X_T)\big]$ by $\mathbb{E}\big[f(\bar{X}_T^n)\big]$ induces the following weak error:

$$\big|\mathbb{E}f(X_T) - \mathbb{E}f(\bar{X}_T^n)\big| \leq \frac{C}{n}$$

with $C = C_{b,\sigma,T} > 0$ and where n is the number of time discretization steps.

From now on, we will drop the exponent n and will denote $\bar{X}$ instead of $\bar{X}^n$.

The estimation of quantities like (4) or (5) can be performed by Monte Carlo simulations since the Euler scheme is simulable. Nevertheless, an alternative to the Monte Carlo method can be to use

cubature formulas produced by an optimal quantization approximation method, especially in small or medium dimension ($d \le 4$ theoretically but, in practice, it may remain competitive with respect to the Monte Carlo method up to dimension $d = 10$, see [18]).

A quantization of an $\mathbb{R}^d$-valued random vector Y induced by a grid $\Gamma \subset \mathbb{R}^d$ is a random vector $\widehat{Y}^\Gamma = \pi(Y)$, where $q : \mathbb{R}^d \to \Gamma$ is a Borel function. Optimal quantization consists in specifying both π and Γ to minimize $\|Y - \widehat{Y}^\Gamma\|_r$ for a given $r \in (0, +\infty)$ (we talk about quadratic optimal quantization when $r = 2$).

Now, suppose that we have access to the optimal quantization or to some "good" (in a sense to be specified further on) quantizations $\big(\widehat{X}_{t_k}^{\Gamma_k}\big)_{k=0,\dots,n}$ (we will sometimes denote $\widehat{X}_{t_k}$ instead of $\widehat{X}_{t_k}^{\Gamma_k}$ to simplify notations) of the process $(\bar{X}_{t_k})_k$ on the grids $\Gamma_k := \Gamma_k^{(N_k)} = \{x_1^k, \dots, x_{N_k}^k\}$ of size N_k (which is also called an N_k-quantizer), for $k = 0, \dots, n$.

If X_0 is random, then we suppose that its distribution can be quantized. In this case $\widehat{X}_0^{\Gamma_0}$ will be the optimal quantization of X_0 of size N_0. If $X_0 = x_0$ is deterministic then $\Gamma_0 = \{x_0\}$ and $\widehat{X}_0^{\Gamma_0} = x_0$.

Suppose as well that we have access to or have computed (offline) the associated weights $\mathbb{P}(\widehat{X}_{t_k}^{\Gamma_k} = x_i^k)$, $i = 1, \dots, N_k$, $k = 0, \dots, n$ (which are the distributions of the $\widehat{X}_{t_k}^{\Gamma_k}$), and the transition probabilities $\widehat{p}_k^{ij} = \mathbb{P}(\widehat{X}_{t_{k+1}}^{\Gamma_{k+1}} = x_j^{k+1} | \widehat{X}_{t_k}^{\Gamma_k} = x_i^k)$ for every $k = 0, \dots, n-1$, $i = 1, \dots, N_k$, $j = 1, \dots, N_{k+1}$ (in other words, the conditional distributions $\mathcal{L}(\widehat{X}_{t_{k+1}}^{\Gamma_{k+1}} | \widehat{X}_{t_k}^{\Gamma_k})$). Then, using optimal quantization cubature formula, the expressions (4) and (5) can be estimated by

$$\mathbb{E}\big[f(\widehat{X}_{t_n}^{\Gamma_n})\big] = \sum_{i=1}^{N_n} f(x_i^n)\, \mathbb{P}\big(\widehat{X}_{t_n}^{\Gamma_n} = x_i^{N_n}\big),$$

since $t_n = T$ and

$$\mathbb{E}\big[f(\widehat{X}_{t_{k+1}}^{\Gamma_{k+1}}) | \widehat{X}_{t_k}^{\Gamma_k} = x_i^k\big] = \sum_{j=1}^{N_{k+1}} \widehat{p}_k^{ij} f(x_j^{k+1}),$$

respectively. The remaining question to be solved is then to know how to get the optimal or at least "good" grids Γ_k, for every $k = 0, \dots, n$, their associated weights and transition probabilities. In a general framework, as soon as the stochastic process $(\bar{X}_{t_k})_k$ (or the underlying diffusion process $(X_t)_{t \ge 0}$ can be simulated one may use zero search stochastic gradient algorithm known as Competitive Learning Vector Quantization (CLVQ), see e.g. [18] or a randomized fixed point procedure (see e.g. [9, 17, 21]) to compute the (hopefully almost) optimal grids and their associated weights or transition probabilities. In the special case of one dimension, we may rely on the deterministic counterpart of these procedures like fugy's algorithm or Lloyd method and, for few specific scalar distributions (the Normal distribution, the exponential distribution, the Weibull distribution, etc), to the Newton-Raphson's algorithm. In this last case, we can speak of fast quantization procedure since this deterministic algorithm leads to more precise estimations and is dramatically faster than stochastic optimization methods. As a typical example of implementation, quadratic optimal quantization grids associated to d-dimensional Normal distribution up to $d = 10$ can be downloaded at the website
www.quantize.math-fi.com.

To highlight the usefulness of our method, suppose for example that we want to price a Put option with a maturity T, a strike K and a present value X_0 in a local volatility model where the dynamics of the stock price process evolves following the stochastic differential equation (called Pseudo-CEV in [11]):

$$dX_t = rX_t dt + \vartheta \frac{X_t^{\delta+1}}{\sqrt{1 + X_t^2}} dW_t, \quad X_0 = x_0, \quad t \in [0, T], \tag{7}$$

where $\delta \in (0, 1)$, $\vartheta \in (0, \underline{\vartheta}]$, $\underline{\vartheta} > 0$, and r stands for the interest rate. In this situation the (unique strong) solution X_T, at time T, is not known analytically and if we want to estimate the quantity of

3

interest: $e^{-rT}\mathbb{E}(f(X_T))$, where $f(x) := \max(K - x, 0)$ is the (Lipschitz continuous) payoff function, we have first of all to discretize the process $(X_t)_{t \in [0,T]}$ as $(\bar{X}_{t_k})_{k=0,\dots,n}$, with $t_n = T$ (using e.g. the Euler scheme), and then estimate

$$e^{-rT}\mathbb{E}(f(\bar{X}_T))$$

by optimal quantization. The only way to produce optimal grids and the associated weights in this situation is to perform stochastic procedures like the CLVQ or randomized Lloyd's procedure (see e.g. [9, 21]), even in the one dimensional framework. However, these methods may be very time consuming. In this framework (as well as in the general local volatility model framework in dimension $d = 1$), our approach allows us to quantize the diffusion process in the Pseudo-CEV model using the Newton-Raphson algorithm. It is important to notice that the companion weights and the probability transitions associated to the quantized process are obtained by a closed formula so that the method involves by no means Monte Carlo simulations. On the other hand, a comparison with Monte Carlo simulation for the pricing of European options in a local volatility model also shows that the proposed method may sometimes be more efficient (with respect to both computational precision and time complexity) than the Monte Carlo method.

The recursive marginal quantization algorithm. Let us be more precise about our proposed method in the general setting where $(X_t)_{t \in [0,T]}$ is a solution to Equation (3). Our aim is in practice to compute the quadratic optimal quantizers $(\Gamma_k)_{0 \le k \le n}$ associated with the Euler scheme $(\bar{X}_{t_k})_{0 \le k \le n}$. Such a sequence (Γ_k) is defined for every $k = 0, \dots, n$ by

$$\Gamma_k \in \operatorname{argmin}\{\bar{D}_k(\Gamma), \Gamma \subset \mathbb{R}^d, \operatorname{card}(\Gamma) \le N_k\}$$

where the function $\bar{D}_k(\cdot)$ is the so-called distortion function associated to $\bar{X}_{t_k}$, and is defined for every N_k-quantizer Γ_k by

$$\bar{D}_k(\Gamma_k) = \mathbb{E}\big|\bar{X}_{t_k} - \widehat{X}_{t_k}^{\Gamma_k}\big|^2 = \mathbb{E}\big(\operatorname{dist}(\bar{X}_{t_k}, \Gamma_k)^2\big),$$

where $\operatorname{dist}(\bar{X}_{t_k}, \Gamma_k)$ is the distance of $\bar{X}_{t_k}$ to Γ_k and $|\cdot|$ is, unless otherwise specified, the Euclidean norm in $\mathbb{R}^d$. At this step, there is no easy way to compute the distortion function $\bar{D}_k(\cdot)$, for $k \ge 1$, because of the form of the density function of $\bar{X}_{t_k}$. However, by conditioning with respect to $\bar{X}_{t_{k-1}}$, we can connect the distortion function $\bar{D}_k(\Gamma_k)$ associated to $\bar{X}_{t_k}$ with the distribution of $\bar{X}_{t_{k-1}}$ by introducing the Euler scheme operator as follows:

$$\bar{D}_k(\Gamma_k) \quad = \quad \mathbb{E}\big[\operatorname{dist}(\mathcal{E}_{k-1}(\bar{X}_{t_{k-1}}, Z_k), \Gamma_k)^2\big] \tag{8}$$

where $(Z_k)_k$ is an $i.i.d.$ sequence of $\mathcal{N}(0; I_q)$-distributed random vectors independent from $\bar{X}_0$ and for every $x \in \mathbb{R}^d$, the Euler operator $\mathcal{E}_{k-1}(x, Z_k)$ is defined by

$$\mathcal{E}_{k-1}(x, Z_k) = x + \Delta b(t_{k-1}, x) + \sqrt{\Delta}\sigma(t_{k-1}, x)Z_k.$$

Now, here is how we construct the algorithm. Given the distribution of $\bar{X}_0$, we quantize $\bar{X}_0$ and denote its quantization by $\widehat{X}_0^{\Gamma_0}$. We want now to define the recursive marginal quantization of $\bar{X}_{t_1}$. Owing to Equation (8) and given that the previous marginal $\bar{X}_0$ has already be quantized, we replace $\bar{X}_0$ by $\widehat{X}_0^{\Gamma_0}$, then, we set $\widetilde{X}_{t_1} := \mathcal{E}_0(\widehat{X}_0^{\Gamma_0}, Z_1)$ and consider the induced distortion

$$\widetilde{D}_1(\Gamma) := \mathbb{E}\big[\operatorname{dist}(\widetilde{X}_{t_1}, \Gamma)^2\big] = \mathbb{E}\big[\operatorname{dist}(\mathcal{E}_0(\widehat{X}_0^{\Gamma_0}, Z_1), \Gamma)^2\big],$$

where $\Gamma \subset \mathbb{R}^d$ and $\operatorname{card}(\Gamma) \le N_1$. The distortion function $\widetilde{D}_1(\cdot)$ is the one to be optimized in order to produce the optimal N_1-quantizer Γ_1. Consequently, we define the recursive marginal quantization of $\bar{X}_{t_1}$ as the optimal quantization $\widehat{X}_{t_1}^{\Gamma_1}$ of $\widetilde{X}_{t_1}$: $\widehat{X}_{t_1}^{\Gamma_1} = \operatorname{Proj}_{\Gamma_1}(\widetilde{X}_{t_1})$, where

$$\Gamma_1 \in \operatorname{argmin}\{\widetilde{D}_1(\Gamma), \ \Gamma \subset \mathbb{R}^d, \ \operatorname{card}(\Gamma) \le N_1\}.$$

4

Once the optimal N_1-quantizer Γ_1 is produced, we define as previously the recursive marginal quantization of $\bar{X}_{t_2}$ as the optimal quantization $\widehat{X}_{t_2}^{\Gamma_2}$ of $\widetilde{X}_{t_1}$ where

$$\Gamma_2 \in \operatorname{argmin}\{\widetilde{D}_2(\Gamma),\ \Gamma \subset \mathbb{R}^d,\ \operatorname{card}(\Gamma) \leq N_2\}$$
$$\widetilde{D}_2(\Gamma) = \mathbb{E}\big[\operatorname{dist}(\widetilde{X}_{t_2},\Gamma)^2\big] \quad \text{and} \quad \widetilde{X}_{t_2} := \mathcal{E}_1(\widehat{X}_1^{\Gamma_1}, Z_2).$$

Repeating this procedure, we define the recursive marginal quantization of $(\bar{X}_{t_k})_{0 \leq k \leq n}$ as the optimal quantizations $(\widehat{X}_{t_k}^{\Gamma_k})_{0 \leq k \leq n}$ of the process $(\widetilde{X}_{t_k})_{0 \leq k \leq n}$: $\forall\, k \in \{0, \ldots, n\}$, $\widehat{X}_{t_k}^{\Gamma_k} = \operatorname{Proj}_{\Gamma_k}(\widetilde{X}_{t_k})$, with $\widetilde{X}_0 = \bar{X}_0$. This leads us to consider the sequence of recursive marginal quantizations $(\widehat{X}_{t_k}^{\Gamma_k})_{k=0,\ldots,N}$ of $(\bar{X}_{t_k})_{k=0,\ldots,N}$, defined from the following recursion:

$$\begin{aligned}
\widetilde{X}_0 &= \bar{X}_0 \\
\widehat{X}_{t_k}^{\Gamma_k} &= \operatorname{Proj}_{\Gamma_k}(\widetilde{X}_{t_k}) \quad \text{and} \quad \widetilde{X}_{t_{k+1}} = \mathcal{E}_k(\widehat{X}_{t_k}^{\Gamma_k}, Z_{k+1}),\ k = 0, \ldots, n-1
\end{aligned}$$

where $(Z_k)_{k=1,\ldots,n}$ is an i.i.d. sequence of $\mathcal{N}(0; I_q)$-distributed random vectors, independent of $\bar{X}_0$.

From an analytical point of view, this approach raises some new challenging problems among which the estimation of the quadratic error bound $\|\bar{X}_{t_k} - \widehat{X}_{t_k}^{\Gamma_k}\|_2 := \big(\mathbb{E}|\bar{X}_{t_k} - \widehat{X}_{t_k}^{\Gamma_k}|_2\big)^{1/2}$, for every $k = 0, \ldots, n$. We will show in particular that for any sequence $(\widehat{X}_{t_k}^{\Gamma_k})_{0 \leq k \leq n}$ of (quadratic) optimal quantization of $(\widetilde{X}_{t_k})_{0 \leq k \leq n}$, the quantization error $\|\bar{X}_{t_k} - \widehat{X}_{t_k}^{\Gamma_k}\|_2$, at the step k of the recursion, is bounded by the cumulative quantization errors $\|\widetilde{X}_{t_i} - \widehat{X}_{t_i}^{\Gamma_i}\|_2$, for $i = 0, \cdots, k$. Owing to the non-asymptotic bound for the quantization errors $\|\widetilde{X}_{t_i} - \widehat{X}_{t_i}^{\Gamma_i}\|_2$, known as Pierce's Lemma (which will be recalled further on in Section 2) we precisely show that for every $k = 0, \ldots, n$, for any $\eta \in]0, 1]$,

$$\|\bar{X}_k - \widehat{X}_k^{\Gamma_k}\|_2 \leq \sum_{\ell=0}^{k} a_\ell N_\ell^{-1/d},$$

where a_ℓ is a positive real constant depending on $b, \sigma, \Delta, x_0, \eta$ (see Theorem 3.1 further on).

The paper is organized as follows. We recall first some basic facts about (regular) optimal quantization in Section 2. The marginal quantization method is described in Section 3. We give in this section the induced quantization error. In section 4, we illustrate how to get the optimal grids using a deterministic zero search Newton-Raphson's algorithm and show how to estimate the associated weights and transition probabilities. The last section, Section 5, is devoted to numerical examples. We first compare the recursive marginal quantization of W_1 with its regular marginal quantization (see Section 2), where $(W_t)_{t \in [0,1]}$ stands for the Brownian motion. Secondly, we use the marginal quantization method for the pricing of an European Put option in a local volatility model (as well as in the Black-Scholes model) and compare the results with those obtained from the Monte Carlo method.

NOTATIONS. We denote by $\mathcal{M}(d, q, \mathbb{R})$ the set of $d \times q$ real-valued matrices. If $A = [a_{ij}] \in \mathcal{M}(d, q, \mathbb{R})$, $A^\star$ denotes its transpose and we define the norm $\|A\| := \sqrt{\operatorname{Tr}(AA^\star)} = (\sum_{i,j} a_{ij}^2)^{1/2}$, where $\operatorname{Tr}(M)$ stands for the trace of M, for $M \in \mathcal{M}(d, d, \mathbb{R})$. For every $g : \mathbb{R}^d \to \mathcal{M}(d, q, \mathbb{R})$, we will set $[g]_{\operatorname{Lip}} = \sup_{x \neq y} \frac{\|g(x) - g(y)\|}{|x - y|}$. For $x, y \in \mathbb{R}$, $x \vee y = \max(x, y)$. For $x \in \mathbb{R}^d$ and $E \subset \mathbb{R}^d$, $\operatorname{dist}(x, E) = \inf_{\xi \in \mathbb{R}^d} |x - \xi|$ (distance of x to E with respect to the current norm $|\,.\,|$ on $\mathbb{R}^d$).

2   Background on optimal quantization

Let $(\Omega, \mathcal{A}, \mathbb{P})$ be a probability space and let $X : (\Omega, \mathcal{A}, \mathbb{P}) \longrightarrow \mathbb{R}^d$ be a random variable with distribution $\mathbb{P}_X$. Assume $\mathbb{R}^d$ is equipped with a norm $|\,.\,|$. Assume $X \in L^r(\mathbb{P})$ i.e. $\|X\|_r := (\mathbb{E}|X|^r)^{1/r} < +\infty$ for a given $r \in (0, +\infty)$ ($\mathbb{E}$ denotes the expectation with respect to $\mathbb{P}$).

The L^r-*optimal quantization problem at level* N for the random vector X (or, in fact, its distribution $\mathbb{P}_X$) consists in finding the best approximation of X in $L^r(\mathbb{P})$ by a function $\pi(X)$ of X where $\pi : \mathbb{R}^d \to \mathbb{R}^d$ is a Borel function taking at most N values. In formalized terms, this amounts out to solve the minimization problem:

$$e_{N,r}(X) = \inf \left\{ \|X - \pi(X)\|_r, \pi : \mathbb{R}^d \to \Gamma, \Gamma \subset \mathbb{R}^d, |\Gamma| \leq N \right\},$$

where $|A|$ stands for the cardinality of a subset $A \subset \mathbb{R}^d$. Note that $e_{N,r}(X)$ only depends on the distribution $\mathbb{P}_X$ of X.

Any $\Gamma = \{x_1, \ldots, x_N\} \subset \mathbb{R}^d$ of size N and any Borel function $\pi : \mathbb{R}^d \to \Gamma$ are both often called N-*quantizer*. The terminology *grid* (or a codebook in coding theory) of size N is more specifically used for Γ itself. The resulting random vector $\pi(X)$ is called an N-*quantization* of X.

Such a grid Γ induces Voronoi diagrams or partitions $(C_i(\Gamma))_{i=1,\ldots,N}$ of $\mathbb{R}^d$ defined as Borel partitions of $\mathbb{R}^d$ satisfying

$$\forall i \in \{1, \cdots, N\}, \quad C_i(\Gamma) \subset \left\{ x \in \mathbb{R}^d : |x - x_i| = \min_{j=1,\ldots,N} |x - x_j| \right\}.$$

To such a Voronoi partition is attached a nearest neighbor projection $\pi_\Gamma = \sum_{i=1}^N x_i \mathbf{1}_{C_i(\Gamma)}$ and a *Voronoi* Γ-*valued quantization* of X denoted $\widehat{X}^\Gamma = \pi_\Gamma(X)$ reading:

$$\widehat{X}^\Gamma = \sum_{i=1}^N x_i \mathbf{1}_{\{X \in C_i(\Gamma)\}}.$$

Then, for any Borel function $\pi : \mathbb{R}^d \to \Gamma$ and any (Borel) nearest neighbor projection π_Γ,

$$|X - \pi(X)| \geq \min_{i=1,\ldots,N} \mathrm{dist}(X, x_i) = \mathrm{dist}(X, \Gamma) = |X - \pi_\Gamma(X)| = |X - \widehat{X}^\Gamma|,$$

so that the optimal L^r-mean quantization error $e_{N,r}(X)$ reads

$$e_{N,r}(X) = \inf \left\{ \|X - \widehat{X}^\Gamma\|_r, \Gamma \subset \mathbb{R}^d, |\Gamma| \leq N \right\} = \inf_{\substack{\Gamma \subset \mathbb{R}^d \\ |\Gamma| \leq N}} \left(\int_{\mathbb{R}^d} \mathrm{dist}(\xi, \Gamma)^r \mathbb{P}_X(d\xi) \right)^{1/r}. \quad (9)$$

Let us recall the following basic facts:

– If $|\,.\,|$ is an Euclidean norm, the boundary of the Voronoi are contained in finitely many hyperplanes so that, if the distribution of X assigns no mass to hyperplanes, two Γ-valued Voronoi quantizations of X are $\mathbb{P}$-*a.s.* equal since they only differ on the boundaries of the Voronoi diagram.

– for every $N \geq 1$, the infimum in (9) is a minimum since it is attained at least at one quantization grid $\Gamma^{N,\star}$ of size at most N. Any resulting $\Gamma^{N,\star}$ is called an L^r-*optimal quantizer at level* N.

– If $|\mathrm{supp}(\mathbb{P}_X))| \geq N$ then any L^r-mean optimal quantizer at level N has exactly full size N (see [10] or [14]).

– The L^r-mean quantization error $e_{N,r}(X)$ decreases to zero as the level N goes to infinity and its sharp rate of convergence is ruled by the so-called Zador Theorem. There is also a non-asymptotic universal upper bound known as Pierce's Lemma. Both results hold for any norm on $\mathbb{R}^d$ and are recalled below. This second result will allow us to put a finishing touch to the proof of our main theoretical result, stated in Theorem 3.1.

Theorem 2.1. (a) **Zador Theorem**, *(see [10]). Let* $r > 0$. *Let* X *be an* $\mathbb{R}^d$-*valued random vector such that* $\mathbb{E}|X|^{r+\eta} < +\infty$ *for some* $\eta > 0$ *and let* $\mathbb{P}_X = f \cdot \lambda_d + P_s$ *be the decomposition of* $\mathbb{P}_X$ *with respect to the Lebesgue measure* λ_d *where* P_s *denotes its singular part. Then*

$$\lim_{N \to +\infty} N^{\frac{1}{d}} e_{N,r}(X) = \widetilde{Q}_r(\mathbb{P}_X) \quad (10)$$

where

$$\widetilde{Q}_r(\mathbb{P}_X) = \widetilde{J}_{r,d}\left(\int_{\mathbb{R}^d} f^{\frac{d}{d+r}}\,d\lambda_d\right)^{\frac{1}{r}+\frac{1}{d}} = \widetilde{J}_{r,d}\,\|f\|_{\frac{d}{d+r}}^{1/r} \in [0,+\infty),$$

$$\widetilde{J}_{r,d} = \inf_{N\geq 1} N^{\frac{1}{d}} e_{N,r}\big(U([0,1]^d)\big) \in (0,+\infty)$$

and $U([0,1]^d)$ *denotes the uniform distribution over the hypercube* $[0,1]^d$.

(b) **Pierce Lemma** *(see [10, 12]). Let* $r,\,\eta > 0$. *There exists a universal constant* $K_{r,d,\eta}$ *such that for every random vector* $X : (\Omega,\mathcal{A},\mathbb{P}) \to \mathbb{R}^d$,

$$\inf_{|\Gamma|\leq N}\|X - \widehat{X}^\Gamma\|_r \leq K_{r,d,\eta}\,\sigma_{r+\eta}(X)N^{-\frac{1}{d}}, \tag{11}$$

where $\sigma_p(X)$ *is the* L^p*-pseudo-standard deviation of* X *defined by*

$$\sigma_p(X) = \inf_{\zeta\in\mathbb{R}^d}\|X - \zeta\|_p \leq +\infty.$$

For more details on the universal contant $K_{2,d,\eta}$, we refer to [12]. We will call $\widetilde{Q}_r(\mathbb{P}_X)$ the Zador's constant associated to X.

From a Numerical Probability viewpoint, finding an optimal N-quantizer Γ may be a challenging task even in the quadratic canonical Euclidean case *i.e.* when $r = 2$ and $|\,.\,|$ is the canonical Euclidean norm on $\mathbb{R}^d$. This framework is the case of interest for numerical applications. The starting point for numerical applications is to note that if we have access to a "good" quantization $\widehat{X}^\Gamma$ close enough to X in distribution, then, for every continuous function $f : \mathbb{R}^d \to \mathbb{R}$, we can approximate $\mathbb{E}f(X)$ (when finite) by the cubature formula:

$$\mathbb{E}f\big(\widehat{X}^\Gamma\big) = \sum_{i=1}^N p_i f(x_i) \tag{12}$$

where $p_i = \mathbb{P}(\widehat{X}^\Gamma = x_i)$, $i = 1,\ldots,N$. By *access* we mean to have numerical values for the grid Γ and its *weights* p_i, $i = 1,\ldots,N$, or equivalently to the distribution of $\widehat{X}^\Gamma$.

Among all good quantizers, the so-called *stationary* quantizers defined below play an important role because they provide higher order cubature formulas (see below) and are also the only class of quantizers that can be reasonably computed owing to its connection with the critical point of the quadratic distortion also defined below.

Definition 2.1. A quantizer $\Gamma = \{x_1,\ldots,x_N\}$ of size N inducing the Voronoi quantization $\widehat{X}^\Gamma$ of X is stationary if

$$
\begin{aligned}
&(i)\ \ \mathbb{P}\left(X \in \cup_i \partial C_i(\Gamma)\right) = 0\\
&(ii)\ \ \mathbb{E}\big(X|\widehat{X}^\Gamma\big) = \widehat{X}^\Gamma\ \ \mathbb{P}\text{-}a.s.
\end{aligned}
\tag{13}
$$

Equation (ii) can be re-written as

$$x_i = \mathbb{E}\big(X\,|\,X \in C_i(\Gamma)\big) = \frac{\mathbb{E}(X\mathbf{1}_{\{X\in C_i(\Gamma)\}})}{\mathbb{P}(X \in C_i(\Gamma))},\ \ i = 1,\ldots,N,$$

with the convention that the equality is always true when $\mathbb{P}(X \in C_i(\Gamma)) = 0$.

This notion of stationarity is closely related to the critical point of the so-called *quadratic distortion* function defined on $(\mathbb{R}^d)^N$ by

$$D_{N,2}(x) = \mathbb{E}\big(\min_{1\leq i\leq N}|X - x_i|^2\big) = \int_{\mathbb{R}^d}|\xi - x_i|^2\mathbb{P}_X(d\xi),\quad x = (x_1,\ldots,x_N)\in(\mathbb{R}^d)^N. \tag{14}$$

This function is clearly symmetric. Its connection with the quadratic mean quantization errors is as follows: set $\Gamma = \{x_i, \ i = 1, \ldots, N\}$ whose cardinality is at most N. Then, with obvious notations,

$$D_{N,2}(x) = \mathbb{E}\big(\mathrm{dist}(X, \Gamma)^2\big) = \int_{\mathbb{R}^d} \mathrm{dist}(\xi, \Gamma)^2 \mathbb{P}_X(d\xi) = \sum_{a \in \Gamma} \int_{C_a(\Gamma)} |\xi - a|^2 \mathbb{P}_X(d\xi).$$

As any grid of size at most N can be "represented" by some N-tuples (by repeating, if necessary, some of its elements), we deduce straightforwardly that

$$e_{N,2}^2(X) = \inf_{(x_1,\ldots,x_N) \in (\mathbb{R}^d)^N} D_{N,2}(x_1, \ldots, x_N).$$

The function $D_{N,2}$ is continuous but also differentiable at any N-tuple having pairwise distinct components with a $\mathbb{P}$-negigible Voronoi partition boundary. The following proposition makes this more precise.

Proposition 2.2. *(see [10, 14]) (a) The function $D_{N,2}$ is differentiable at any N-tuple $(x_1, \ldots, x_N) \in (\mathbb{R}^d)^N$ having pairwise distinct components and such that $\mathbb{P}\left(X \in \cup_i \partial C_i(\Gamma)\right) = 0$. Furthermore, we have*

$$\nabla D_{N,2}(x_1, \ldots, x_N) \ = \ 2\Big(\int_{C_i(\Gamma)} (x_i - x) d\mathbb{P}_X(x)\Big)_{i=1,\ldots,N} \tag{15}$$

$$= \ 2\Big(\mathbb{P}(X \in C_i(\Gamma))x_i - \mathbb{E}(X\mathbf{1}_{\{X \in C_i(\Gamma)\}})\Big)_{i=1,\ldots,N}. \tag{16}$$

(b) A grid $\Gamma = \{x_1, \ldots, x_N\}$ of full size N is stationary if and only if

$$\mathbb{P}\left(X \in \cup_i \partial C_i(\Gamma)\right) = 0 \quad \text{and} \quad \nabla D_{N,2}(\Gamma) = 0. \tag{17}$$

(c) If the support of $\mathbb{P}_X$ has at least N elements, any L^2-optimal quantizer at level N has full size and a $\mathbb{P}$-negligible Voronoi boundary. Hence it is a stationary N-quantizer.

CONVENTION: To alleviate notations, we will often put grids of all size N as an argument of the distortion function $D_{2,N}$ as well as for its gradient when its Voronoi boundary is negligible. This has already been done implicitly in the introduction.

When approximating $\mathbb{E}f(X)$ by $\mathbb{E}f(\widehat{X}^\Gamma)$ and f is smooth enough (say $\mathcal{C}^{1+\alpha}$) and Γ is a stationary N-quantizer, the resulting error may be bounded by the quantization error $\|X - \widehat{X}^\Gamma\|_2$. We briefly recall some error bounds induced from the approximation of $\mathbb{E}f(X)$ by (12) (we refer to [18] for further details).

(a) Let Γ be a stationary quantizer and let f be a Borel function on $\mathbb{R}^d$. If f is a convex function then

$$\mathbb{E}f(\widehat{X}^\Gamma) \le \mathbb{E}f(X). \tag{18}$$

(b) Lipschitz continuous functions:

– If f is Lipschitz continuous then for any N-quantizer Γ we have

$$\big|\mathbb{E}f(X) - \mathbb{E}f(\widehat{X}^\Gamma)\big| \le [f]_{\mathrm{Lip}}\|X - \widehat{X}^\Gamma\|_2.$$

– Let $\theta : \mathbb{R}^d \to \mathbb{R}_+$ be a nonnegative convex function such that $\theta(X) \in L^2(\mathbb{P})$. If f is locally Lipschitz with at most θ-growth, i.e. $|f(x) - f(y)| \le [f]_{\mathrm{Lip}}|x - y|(\theta(x) + \theta(y))$ then $f(X) \in L^1(\mathbb{P})$ and

$$\big|\mathbb{E}f(X) - \mathbb{E}f(\widehat{X}^\Gamma)\big| \le 2[f]_{\mathrm{Lip}}\|X - \widehat{X}^\Gamma\|_2 \|\theta(X)\|_2.$$

(c) Differentiable functions: if f is differentiable on $\mathbb{R}^d$ with an α-Hölder gradient ∇f ($\alpha \in [0, 1]$), then for any stationary N-quantizer Γ,

$$\left|\mathbb{E}f(X) - \mathbb{E}f(\widehat{X}^\Gamma)\right| \leq [\nabla f]_{\alpha,\mathrm{Hol}}\|X - \widehat{X}^\Gamma\|_2^{1+\alpha}.$$

3 Recursive marginal quantization of the Euler process

Let $(X_t)_{t\geq 0}$ be a stochastic process taking values in a d-dimensional Euclidean space $\mathbb{R}^d$ and solution to the stochastic differential equation:

$$dX_t = b(t, X_t)dt + \sigma(t, X_t)dW_t, \quad X_0 \in \mathbb{R}^d, \tag{19}$$

where W is a standard q-dimensional Brownian motion starting at 0 and where $b : [0, T] \times \mathbb{R}^d \to \mathbb{R}^d$ and the matrix diffusion coefficient function $\sigma : [0, T] \times \mathbb{R}^d \to \mathcal{M}(d, q, \mathbb{R})$ are measurable and satisfy

$$b(., 0) \quad \text{and} \quad \sigma(., 0) \quad \text{are bounded on} \quad [0, T] \tag{20}$$

and the uniform global Lipschitz continuity assumption : for every $t \in [0, T]$ and every $x \in \mathbb{R}^d$,

$$|b(t, x) - b(t, y)| \leq [b]_{\mathrm{Lip}}|x - y| \quad \text{and} \quad \|\sigma(t, x) - \sigma(t, y)\| \leq [\sigma]_{\mathrm{Lip}}|x - y|. \tag{21}$$

In particular, this implies that

$$|b(t, x)| \leq L(1 + |x|) \quad \text{and} \quad \|\sigma(t, x)\| \leq L(1 + |x|) \tag{22}$$

with $L = \max\left([b]_{\mathrm{Lip}}, \|b(., 0)\|_{\mathrm{sup}}, [\sigma]_{\mathrm{Lip}}, \|\sigma(., 0)\|_{\mathrm{sup}}\right)$. These assumptions guarantee the existence of a unique strong solution of (19) starting from any $x_0 \in \mathbb{R}^d$.

3.1 The algorithm

Consider the Euler scheme of the process $(X_t)_{t\geq 0}$ starting from $\bar{X}_0 = X_0$:

$$\bar{X}_{t_{k+1}} = \bar{X}_{t_k} + \Delta b(t_k, \bar{X}_{t_k}) + \sigma(t_k, \bar{X}_{t_k})(W_{t_{k+1}} - W_{t_k}),$$

where $t_k = \frac{kT}{n} = k\Delta$ for every $k \in \{0, \ldots, n\}$.

NOTATION SIMPLIFICATION. To alleviate notations, we set

$$Y_k := Y_{t_k} \text{ (for any process } Y \text{ evaluated at time } t_k)$$
$$b_k(x) := b(t_k, x), \quad x \in \mathbb{R}^d$$
$$\sigma_k(x) := \sigma(t_k, x), \quad x \in \mathbb{R}^d.$$

Recall that the distortion function $\bar{D}_k$ associated to $\bar{X}_k$ may be written for every $k = 0, \ldots, n-1$, as

$$\bar{D}_{k+1}(\Gamma_{k+1}) = \mathbb{E}\left[\mathrm{dist}(\mathcal{E}_k(\bar{X}_k, Z_{k+1}), \Gamma_{k+1})^2\right]$$

where

$$\mathcal{E}_k(x, z) := x + \Delta b(t_k, x) + \sqrt{\Delta}\sigma(t_k, x)z, \ x \in \mathbb{R}^d, \ z \in \mathbb{R}^q.$$

Supposing that $\bar{X}_0$ has already been quantized by $\widehat{X}_0^{\Gamma_0}$ and setting $\widetilde{X}_1 = \mathcal{E}_0(\widehat{X}_0^{\Gamma_0}, Z_1)$, we may approximate the distortion function $\bar{D}_1(\Gamma_1)$ by

$$
\begin{aligned}
\widetilde{D}_1(\Gamma_1) &:= \mathbb{E}\big[\mathrm{dist}(\widetilde{X}_1, \Gamma_1)^2\big] \\
&= \mathbb{E}\big[\mathrm{dist}(\mathcal{E}_0(\widehat{X}_0^{\Gamma_0}, Z_1), \Gamma_1)^2\big] \\
&= \sum_{i=1}^{N_0} \mathbb{E}\big[\mathrm{dist}(\mathcal{E}_0(x_i^0, Z_1), \Gamma_1)^2\big]\mathbb{P}\big(\widehat{X}_0^{\Gamma_0} = x_i^0\big).
\end{aligned}
$$

This allows us (as already said in the introduction) to consider the sequence of recursive (marginal) quantizations $(\widehat{X}_k^{\Gamma_k})_{k=0,\ldots,n}$ defined from the following recursion:

$$
\widehat{X}_k^{\Gamma_k} = \mathrm{Proj}_{\Gamma_k}(\widetilde{X}_k) \quad \text{and} \quad \widetilde{X}_k = \mathcal{E}_k(\widehat{X}_{k-1}^{\Gamma_k}, Z_k), \; k = 1, \ldots, n, \; \widetilde{X}_0 = \bar{X}_0. \tag{23}
$$

where $(Z_k)_{k=1,\ldots,n}$ is an i.i.d., sequence of $\mathcal{N}(0; I_q)$-distributed random vectors, independent of $\bar{X}_0$.

3.2 The error analysis

Our aim is now to compute the quantization error bound $\|\bar{X}_T - \widehat{X}_T\|_2 := \|\bar{X}_n - \widehat{X}_n^{\Gamma_n}\|_2$. The analysis of this error bound will be the subject of the following theorem, which is the main result of the paper. In this section, we assume for convenience that $\widetilde{X}_0 = X_0 = x_0$ (which amounts to conditioning with respect to $\sigma(X_0)$ since W and X_0 are independent).

Theorem 3.1. *Let the coefficients b, σ satisfy the assumptions (20) and (21). Let for every $k = 0, \ldots, n$, Γ_k be a quadratic optimal quantizer for $\widetilde{X}_k$ at level N_k. Then, for every $k = 0, \ldots, n$, for any $\eta \in (0, 1]$,*

$$
\|\bar{X}_k - \widehat{X}_k^{\Gamma_k}\|_2 \leq K_{2,d,\eta} \sum_{\ell=1}^{k} a_\ell(b, \sigma, t_k, \Delta, x_0, L, 2 + \eta) N_\ell^{-1/d} \tag{24}
$$

where $K_{2,d,\eta}$ is a universal constant defined in Equation (11) and, for every $p \in (2, 3]$,

$$
a_\ell(b, \sigma, t_k, \Delta, x_0, L, p) := e^{C_{b,\sigma}\frac{(t_k - t_\ell)}{p}} \left[e^{(\kappa_p + K_p)t_\ell}|x_0|^p + \frac{e^{\kappa_p \Delta}L + K_p}{\kappa_p + K_p}\left(e^{(\kappa_p + K_p)t_\ell} - 1\right) \right]^{\frac{1}{p}}
$$

with $C_{b,\sigma} = [b]_{\mathrm{Lip}} + \frac{1}{2}[\sigma]_{\mathrm{Lip}}^2$, $\kappa_p := \frac{(p-1)(p-2)}{2} + 2pL$ and $K_p := 2^{p-1}L^p\left(1 + p + \Delta^{\frac{p}{2}-1}\right)\mathbb{E}|Z|^p$, $Z \sim \mathcal{N}(0; I_q)$.

Let us make the following remarks.

Remark 3.1. It is crucial for applications to notice that the real constants $a_\ell(\cdot, t_k, \cdot, \cdot, \cdot, \cdot, p)$ do not explode when n goes to infinity and we have

$$
\sup_{n \geq 1} \max_{0 \leq \ell \leq k \leq n} a_\ell(\cdot, t_k, \cdot, \cdot, \cdot, \cdot, p) \leq e^{C_{b,\sigma}\frac{T}{p}} \left[e^{(\kappa_p + K_p^\star)T}|x_0|^p + \frac{e^{\kappa_p T}L + K_p^\star}{\kappa_p}\left(e^{(\kappa_p + K_p^\star)T} - 1\right) \right]^{\frac{1}{p}},
$$

where $K_p^\star = 2^{p-1}L^p\left(1 + p + T^{\frac{p}{2}-1}\right)$. We also remark that $\kappa_p \leq 2(1 + p)L$.

The proof of the theorem relies on the Lemma below, which proof is postponed to the appendix.

Lemma 3.2. *Let the coefficients b, σ of the diffusion satisfy the assumptions* (20) *and* (21). *Then, for every $p \in (2,3]$, for every $k = 0, \ldots, n$,*

$$\mathbb{E}|\widetilde{X}_k|^p \le e^{(\kappa_p + K_p)t_k}|x_0|^p + \frac{e^{\kappa_p \Delta}L + K_p}{\kappa_p + K_p}\left(e^{(\kappa_p + K_p)t_k} - 1\right), \tag{25}$$

where K_p and κ_p are defined in Theorem 3.1.

Let us prove the theorem.

Proof *(of Theorem 3.1).* First we note that for every $k = 0, \ldots, n$,

$$\|\bar{X}_k - \widehat{X}_k\|_2 \le \|\bar{X}_k - \widetilde{X}_k\|_2 + \|\widetilde{X}_k - \widehat{X}_k^{\Gamma_k}\|_2. \tag{26}$$

Let us control the first term of the right hand side of the above equation. To this end, we first note that, for every $k = 0, \ldots, n$, the function $\mathcal{E}_k(\cdot, Z_{k+1})$ is Lipschitz w.r.t. the L^2-norm: in fact, for every $x, x' \in \mathbb{R}^d$,

$$\begin{aligned}
\mathbb{E}|\mathcal{E}_k(x, Z_{k+1}) - \mathcal{E}_k(x', Z_{k+1})|^2 &\le \left(1 + \Delta\left(2[b_k]_{\mathrm{Lip}} + [\sigma_k]_{\mathrm{Lip}}^2\right) + \Delta^2[b_k(.)]_{\mathrm{Lip}}^2\right)|x - x'|^2 \\
&\le \left(1 + \Delta\left(2[b]_{\mathrm{Lip}} + [\sigma]_{\mathrm{Lip}}^2\right) + \Delta^2[b]_{\mathrm{Lip}}^2\right)|x - x'|^2 \\
&\le (1 + \Delta C_{b,\sigma})^2|x - x'|^2 \\
&\le e^{2\Delta C_{b,\sigma}}|x - x'|^2,
\end{aligned}$$

where $C_{b,\sigma} = [b]_{\mathrm{Lip}} + \frac{1}{2}[\sigma]_{\mathrm{Lip}}^2$ does not depend on n. Then, it follows that for every $\ell = 0, \ldots, k-1$,

$$\begin{aligned}
\|\bar{X}_{\ell+1} - \widetilde{X}_{\ell+1}\|_2 &= \|\mathcal{E}_\ell(\bar{X}_\ell, Z_{\ell+1}) - \mathcal{E}_\ell(\widehat{X}_\ell^{\Gamma_\ell}, Z_{\ell+1})\|_2 \\
&\le e^{\Delta C_{b,\sigma}}\|\bar{X}_\ell - \widehat{X}_\ell^{\Gamma_\ell}\|_2 \\
&\le e^{\Delta C_{b,\sigma}}\|\bar{X}_\ell - \widetilde{X}_\ell\|_2 + e^{\Delta C_{b,\sigma}}\|\widetilde{X}_\ell - \widehat{X}_\ell^{\Gamma_\ell}\|_2.
\end{aligned} \tag{27}$$

Then, we show by a backward induction using (26) and (27) that (recall that $\widetilde{X}_0 = \widehat{X}_0^{\Gamma_0} = x_0$)

$$\|\bar{X}_k - \widetilde{X}_k\|_2 \le \sum_{\ell=1}^{k} e^{(k-\ell)\Delta C_{b,\sigma}}\|\widetilde{X}_\ell - \widehat{X}_\ell^{\Gamma_\ell}\|_2.$$

Now, we deduce from Pierce's Lemma (Equation 11 in Theorem 2.1(b)) and Lemma 3.2 that, for every $k = 0, \ldots, n$, for any $\eta \in]0, 1]$,

$$\begin{aligned}
\|\bar{X}_k - \widehat{X}_k\|_2 &\le K_{2,d,\eta}\sum_{\ell=1}^{k} e^{(k-\ell)\Delta C_{b,\sigma}}\sigma_{2,\eta}(\widetilde{X}_\ell)N_\ell^{-1/d} \\
&\le K_{2,d,\eta}\sum_{\ell=1}^{k} e^{(k-\ell)\Delta C_{b,\sigma}}\|\widetilde{X}_\ell\|_{2+\eta}N_\ell^{-1/d} \\
&\le K_{2,d,\eta}\sum_{\ell=1}^{k} a_\ell(b, \sigma, t_k, \Delta, x_0, L, 2+\eta)N_\ell^{-1/d},
\end{aligned}$$

which is the announced result. $\qquad\square$

PRACTITIONER'S CORNER. (a) *Optimal dispatching (to minimize the error bound).* When we consider the upper bound of Equation (24), a natural question is to determine how to dispatch optimally

the sizes $N_1, \cdots, N_n$ (for a fixed mesh of length n) of the quantization grids when we wish to use a total "budget" $N = N_1 + \cdots + N_n$ of elementary quantizers (with $N_k \geq 1$, for every $k = 1, \ldots, n$). Keep in mind that since X_0 is not random, $N_0 = 1$. The dispatching problem amounts to solving the minimization problem

$$\min_{N_1 + \cdots + N_n = N} \sum_{\ell=1}^{n} a_\ell N_\ell^{-1/d}$$

where $a_\ell = a_\ell(b, \sigma, t_n, \Delta, x_0, L, 2 + \eta)$. This leads (see e.g. [1]) to the following optimal dispatching: for every $\ell = 1, \ldots, n$,

$$N_\ell = \left\lfloor \frac{a_\ell^{\frac{d}{d+1}}}{\sum_{k=1}^{n} a_k^{\frac{d}{d+1}}} N \right\rfloor \vee 1,$$

so that Equation (24) becomes at the terminal instant n:

$$\|\bar{X}_n - \widehat{X}_n^{\Gamma_n}\|_2 \lesssim K_{2,d,\eta} N^{-1/d} \Big(\sum_{\ell=1}^{n} a_\ell^{\frac{d}{d+1}} \Big)^{1+1/d}. \tag{28}$$

(*b*) *Uniform dispatching (complexity minimization).* Notice that the complexity of the quantization tree $(\Gamma_k)_{k=0,\ldots,N}$ for the recursive marginal quantization is of order $\sum_{k=0}^{n-1} N_k N_{k+1}$. Now, assuming that $N_0 = 1$ and that for every $N_k \leq N_{k+1}$, $k = 0, \ldots, n-1$, we want to solve (heuristically) the problem

$$\min \Big\{ \sum_{k=0}^{n-1} N_k N_{k+1} \text{ subject to } \sum_{k=1}^{n} N_k = N \Big\}. \tag{29}$$

As $\sum_{k=0}^{n-1} N_k^2 \leq \sum_{k=0}^{n-1} N_k N_{k+1} \leq \sum_{k=1}^{n} N_k^2$ and $N_0 = 1$, this suggests that $\sum_{k=0}^{n-1} N_k N_{k+1} \approx \sum_{k=1}^{n} N_k^2$. Then, if we switch to

$$\min \Big\{ \sum_{k=1}^{n} N_k^2/N^2 \text{ subject to } \sum_{k=1}^{n} N_k = N \Big\} = \min \Big\{ \sum_{k=1}^{n} q_k^2 \text{ subject to } \sum_{k=1}^{n} q_k = 1 \Big\}, \tag{30}$$

where $q_k = N_k/N$, it is well known that the solution of this problem is given by $q_k = 1/n$, *i.e.*, $N_k = N/n$, for every $k = 1, \ldots, n$. Plugging this in (29), leads to a sub-optimal, but nearly optimal, complexity equal to N^2/n. In fact, any other choice leads to the global complexity

$$N^2 \sum_{k=0}^{n-1} q_k q_{k+1} \geq N^2 \sum_{k=0}^{n-1} q_k^2 \geq N^2 \min \Big\{ \sum_{k=0}^{n} q_k^2 \text{ subject to } \sum_{k=0}^{n} q_k = 1 \Big\} > \frac{N^2}{n}$$

(provided q_0 is left free).

(*c*) *Comparison.* If we consider the uniform dispatching $N_\ell = \bar{N} := N/n$, $\ell = 1, \ldots, n$, the error bound in Theorem 3.1 becomes, still at at the terminal instant,

$$\|\bar{X}_n - \widehat{X}_n^{\Gamma_n}\|_2 \lesssim K_{2,d,\eta} \Big(\frac{n}{N} \Big)^{1/d} \sum_{\ell=1}^{n} a_\ell. \tag{31}$$

It is clear that the upper bound (28) is a sharper bound than (31) since, by Hölder's Inequality,

$$\Big(\sum_{\ell=1}^{n} a_\ell^{\frac{d}{d+1}} \Big)^{1+1/d} < n^{1/d} \sum_{\ell=1}^{n} a_\ell.$$

However, the uniform dispatching has smaller complexity than the optimal one.

4 Computation of the marginal quantizers

We focus now on the numerical computation of the quadratic optimal quantizers of the marginal random variable $\widetilde{X}_{t_{k+1}}$ given the probability distribution function of $\widetilde{X}_{t_k}$. Such a task requires the use of some algorithms like the CLVQ algorithm, the randomized Lloyd's algorithms (both requiring the computation of the gradient of the distortion function) or Newton-Raphson's algorithm (especially for the one-dimensional setting) which involves the gradient and the Hessian matrix of the distortion (we refer to [18] for more details). To ensure the existence of densities (or conditional densities) of the $\widetilde{X}_{t_{k+1}}$'s (given $\widetilde{X}_{t_k}$), we suppose that the matrix $\sigma\sigma^\star(t,x)$ is invertible for every $(t,x)\in[0,T]\times\mathbb{R}^d$.

For every $k\in\{0,\ldots,n\}$, let $\widehat{X}_k^\Gamma$ be the quantization of $\widetilde{X}_k$ induced by a grid $\Gamma\subset\mathbb{R}^d$. Recall that the distortion function at level $N_k\in\mathbb{N}$ attached to $\widetilde{X}_k$ is defined on $(\mathbb{R}^d)^{N_k}$ by

$$\widetilde{D}_k(x) = \mathbb{E}\min_{1\leq i\leq N_k}|\widetilde{X}_k - x_i|^2 = \int \min_{1\leq i\leq N_k}|\xi - x_i|^2\mathbb{P}_{\widetilde{X}_k}(d\xi), \quad x = (x_1,\ldots,x_{N_k})\in(\mathbb{R}^d)^{N_k}$$

having in mind that, if $\Gamma_x = \{x_i, i = 1,\ldots,N_k\}$, then $\widetilde{D}_k(x) = \|\widetilde{X}_k - \widehat{X}_k^{\Gamma_x}\|_2^2$.

Our aim is to compute the (at least locally) optimal quadratic quantization grids $(\Gamma_k)_{k=0,\ldots,n}$ associated with the random vectors $\widetilde{X}_k$, $k = 0,\ldots,n$. Such a sequence of grids is defined for every $k = 0,\ldots,n$ by

$$\Gamma_k \in \mathrm{argmin}\left\{\|\widehat{X}_k^\Gamma - \widetilde{X}_k\|_2, \Gamma\subset\mathbb{R}^d, \mathrm{card}(\Gamma)\leq N_k\right\} = \mathrm{argmin}\left\{\widetilde{D}_k(x),\, x\in(\mathbb{R}^d)^{N_k}\right\} \tag{32}$$

where the sequence of (marginal) quantizations $(\widetilde{X}_k)_{k=0,\ldots,N}$ is recursively defined by (23):

$$\widetilde{X}_k = \mathcal{E}_k(\widehat{X}_{k-1}, Z_k),\ \widehat{X}_{k-1} = \mathrm{Proj}_{\Gamma_{k-1}}(\widetilde{X}_{k-1}),\ k = 1,\ldots,n,\ \widetilde{X}_0 = \bar{X}_0,$$

where $(Z_k)_{k=1,\ldots,n}$ is an i.i.d. sequence of $\mathcal{N}(0; I_q)$-distributed random vectors, independent of $\bar{X}_0$.

By observing the above recursion and the optimization problem (32), we see that the optimal grids Γ_k are defined *recursively* (which is not the case for regular marginal quantization developed in former works). At this point the interesting fact which motivates the whole approach is that the distortion function at time $k+1$, $\widetilde{D}_{k+1}$, $k = 0,\ldots,n-1$, can in turn be written recursively from the grid Γ_k already optimized at time k and the distortion function of Normal distribution.

Let $D_N^{m,\Sigma}$ be the distortion function of the $\mathcal{N}(m;\Sigma)$-distribution defined on $(\mathbb{R}^d)^N$ by

$$D_N^{m,\Sigma}(x) = \mathbb{E}\min_{1\leq i\leq N}|\Sigma Z + m - x_i|^2.$$

As $\widetilde{X}_k$ has already been (optimally) quantized by a grid $\Gamma_k = \{x_1^k,\ldots,x_{N_k}^k\}$ to which are attached the weights

$$p_i^k = \mathbb{P}(\widehat{X}_k = x_i^k),\ i = 1,\ldots,N_k,$$

we derive from (23) that, for every $x^{k+1}\in(\mathbb{R}^d)^{N_{k+1}}$,

$$\begin{aligned}
\widetilde{D}_{k+1}(x^{k+1}) &= \mathbb{E}\left[\mathrm{dist}(\mathcal{E}_k(\widehat{X}_k, Z_{k+1}), x^{k+1})^2\right] \\
&= \sum_{i=1}^{N_k}\mathbb{E}\left[\mathrm{dist}(\mathcal{E}_k(x_i^k, Z_{k+1}), x^{k+1})^2\right]\mathbb{P}(\widehat{X}_k = x_i^k) \\
&= \sum_{i=1}^{N_k} p_i^k D_{N_{k+1}}^{m_i^k,\Sigma_i^k}(x^{k+1})
\end{aligned}$$

since $\mathcal{E}_k(x_i^k, Z_{k+1}) \stackrel{d}{=} \mathcal{N}(m_i^k; \Sigma_i^k)$ with

$$m_i^k = x_i^k + \Delta b(t_k, x_i^k) \quad \text{and} \quad \Sigma_i^k = \sqrt{\Delta}\sigma(t_k, x_i^k), \ k = 0, \dots, n.$$

Then, owing to Proposition 2.2, the distortion function $\widetilde{D}_{k+1}$ is continuously differentiable as a function of the N_{k+1}-tuple x^{k+1} with pairwise distinct components. This follows from the fact that the distortion functions $D_{N_{k+1}}^{m,\Sigma}$ are differentiable at such a N_{k+1}-tuple as soon as $\Sigma\Sigma^*$ is positive and definite.

Its gradient is given by

$$
\begin{aligned}
\nabla\widetilde{D}_{k+1}(x^{k+1}) &= 2\Big(\sum_{i=1}^{N_k} p_i^k \frac{\partial D_{N_{k+1}}^{m_i^k, \Sigma_i^k}(x^{k+1})}{\partial x_j^{k+1}}\Big)_{j=1,\dots,N_{k+1}} \\
&= 2\Big(\mathbb{E}\Big[\sum_{i=1}^{N_k} p_i^k\Big(\mathbf{1}_{\{\mathcal{E}_k(x_i^k, Z_{k+1}) \in C_j(\Gamma_{k+1})\}}\big(x_j^{k+1} - \mathcal{E}_k(x_i^k, Z_{k+1})\big)\Big]\Big)_{j=1,\dots,N_{k+1}} \quad (33)
\end{aligned}
$$

Remark 4.1. If Γ_{k+1} is a quadratic optimal N_{k+1}-quantizer for $\widetilde{X}_{k+1}$ and if $\widehat{X}_{k+1}^{\Gamma_{k+1}}$ denotes the quantization of $\widetilde{X}_{k+1}$ by the grid Γ_{k+1}, then $\nabla\widetilde{D}_{k+1}(\Gamma_{k+1}) = 0$ and Γ_{k+1} is a stationary quantizer, for $\widetilde{X}_{k+1}$ i.e. $\mathbb{E}\big(\widetilde{X}_{k+1}\big|\widehat{X}_{k+1}\big) = \widehat{X}_{k+1}$ or equivalently $\Gamma_{k+1} = \{x_i^{k+1}, \ i = 1, \dots, N_{k+1}\}$ with

$$x_j^{k+1} = \frac{\sum_{i=1}^{N_k} p_i^k \mathbb{E}\big(\mathcal{E}_k(x_i^k, Z_{k+1})\mathbf{1}_{\{\mathcal{E}_k(x_i^k, Z_{k+1}) \in C_j(\Gamma_{k+1})\}}\big)}{p_j^{k+1}} \quad (34)$$

$$\text{and} \qquad p_j^{k+1} = \sum_{i=1}^{k} p_i^k \mathbb{P}\big(\mathcal{E}_k(x_i^k, Z_{k+1}) \in C_j(\Gamma_{k+1})\big), \ j = 1, \dots, N_{k+1}. \quad (35)$$

APPLICATION TO THE COMPUTATION OF THE GRIDS. It follows from the stationarity Equations (33) on the one hand and (34) and (35) on the other hand that one can compute by a *zero search* stochastic gradient descent (known as CLVQ) or a randomized *fixed point* Lloyd algorithm time in a step by time step forward induction. In both cases, we are not only interested in the grids but by the whole distribution of $\widetilde{X}_k$ so we need to implement a companion procedure to compute the weights p_i^k. Put in a different way, this simply means that the distribution of the random vectors $\widetilde{X}_k$ can be simulated recursively.

However, in view of our applications, we need much more than these distributions: though the sequence $(\widehat{X}_k)_{k=0,\dots,n}$ is not a Markov chain we need all its transitions $\mathcal{L}\big(\widehat{X}_{k+1}\,\big|\,\widehat{X}_k\big)$, $k = 0, \dots, n-1$, namely

$$
\begin{aligned}
p_{ij}^k &= \mathbb{P}\big(\widehat{X}_{k+1} \in C_j(\Gamma_{k+1})|\widehat{X}_k \in C_i(\Gamma_k)\big) = \mathbb{P}\big(\widetilde{X}_{k+1} \in C_j(\Gamma_{k+1})|\widetilde{X}_k \in C_i(\Gamma_k)\big) \\
&= \mathbb{P}\big(\mathcal{E}_k(x_i^k, Z_{k+1}) \in C_j(\Gamma_{k+1})\big), \quad i \in \{1, \dots, N_k\}, \ j \in \{1, \dots, N_{k+1}\}. \quad (36)
\end{aligned}
$$

Looking back at (35), it is clear that, whatever the adopted method is, these quantities are to be computed in the above procedure to have access to p_j^{k+1} (this is but Bayes' formula).

This optimization phase which is crucial for applications can become time consuming as the dimension d grows since it relies *in fine* on Monte Carlo simulations based on nearest neighbor searches. In fact when d is larger than 3 or 4 a variant should be devised to make the procedure reasonably fast (see [20]). In fact all the above formulas can be expressed as d-dimensional integrals over (convex) Voronoi cells. In dimension 1, 2 or possibly 3 it can be still possible to compute some of such integrals (see Qhull website: www.qhull.org).

In the section below, we detail a 1-dimensional version which turns out to be extremely fast in practice, since it take advantage of the Newton-Raphson algorithm to perform a zero search procedure for $\nabla \widetilde{D}_k$.

4.1 The one dimensional setting

In a dimensional setting, we can canonically represent a grid $\Gamma = \{x_1, \ldots, x_N\}$ of full size N by a unique N-tuple with increasing components $(x_1, \ldots, x_N)$. So from now on in this section, we will always make the abuse of notation that the symbol Γ will denote the N-tuple of its values in increasing order.

4.1.1 Computing marginal quantizers with Newton-Raphson algorithm

It is a well-known fact that if a distribution μ has a continuous density the resulting distortion functions D_N^μ are in fact twice differentiable at N-tuples with pairwise distinct components and negligible Voronoi diagram boundary, with an explicit, though rather involved, expression (see *e.g.* [21]). So, as the distortion functions $D_N^{m,\Sigma}$ associated to the $\mathcal{N}(m; \Sigma)$ are twice differentiable, in turn the distortion function of $\widetilde{D}_{k+1}$ is twice differentiable. Hence it is possible, at least formally, to write down a Newton-Raphson zero search procedure, indexed by $\ell \in \mathbb{N}$, where a current grid $\Gamma_{k+1}^{(\ell)}$ is updated as follows:

$$\Gamma_{k+1}^{(\ell+1)} = \Gamma_{k+1}^{(\ell)} - \big(\nabla^2 \widetilde{D}_{k+1}(\Gamma_{k+1}^{(\ell)})\big)^{-1} \nabla \widetilde{D}_{k+1}(\Gamma_{k+1}^{(\ell)}), \quad \ell \geq 0, \tag{37}$$

starting from a $\Gamma^{(0)} \in \mathbb{R}^{N_{k+1}}$ (with increasing components). Of course, $\nabla \widetilde{D}_k(\Gamma_k)$ and $\nabla^2 \widetilde{D}_k(\Gamma_k)$ denote respectively the gradient vector and the Hessian matrix of the distortion function $\widetilde{D}_k$.

To this end we need a closed form for the Hessian $\nabla^2 \widetilde{D}_{k+1}$ of $\widetilde{D}_{k+1}$. We will rely on the expression (33) for the gradient $\nabla \widetilde{D}_{k+1}$ and take advantage of the fact that it can be reduced to the gradient of the distortion function of a Gaussian $m + \sqrt{v}Z$, $Z \stackrel{d}{=} \mathcal{N}(0; 1)$. We will denote by Φ_0 and Φ_0' the cumulative distribution function and the probability density function of the $\mathcal{N}(0; 1)$ distribution respectively and we will extensively take advantage of the obvious fact

$$\int_{-\infty}^{x} \xi \Phi_0'(\xi) d\xi = -\Phi_0'(x), \ x \in \mathbb{R}.$$

To simplify notation, set for every $k = 0, \ldots, n-1$ and every $j = 1, \ldots, N_{k+1}$,

$$x_{j-1/2}^{k+1} = \frac{x_j^{k+1} + x_{j-1}^{k+1}}{2}, \ x_{j+1/2}^{k+1} = \frac{x_j^{k+1} + x_{j+1}^{k+1}}{2}, \ \text{with } x_{1/2}^{k+1} = -\infty, x_{N_{k+1}+1/2}^{k+1} = +\infty,$$

and let us define for every $\xi \in \mathbb{R}$, $v_k(\xi) = \sqrt{\Delta}\sigma_k(\xi)$, $m_k(\xi) = x + \Delta b_k(\xi)$,

$$x_{j-}^{k+1}(\xi) := \frac{x_{j-1/2}^{k+1} - m_k(\xi)}{v_k(\xi)} \quad \text{and} \quad x_{j+}^{k+1}(\xi) := \frac{x_{j+1/2}^{k+1} - m_k(\xi)}{v_k(\xi)}, \ k = 0, \ldots, n-1.$$

Let $\Gamma_{k+1} = (x^{k+1}, \ldots, x_{N_{k+1}}^{k+1}) \in \mathbb{R}^{N_{k+1}}$ (we temporarily drop the dependence of all the grid points in ℓ to alleviate notations). Also have in mind that $p_i^k = \mathbb{P}(\widehat{X}_k = x_i^k)$. Then, for every $j = 1, \ldots, N_{k+1}$

$$\frac{\partial \widetilde{D}_{k+1}(\Gamma_{k+1})}{\partial x_j^{k+1}} = \sum_{i=1}^{N_k} p_i^k \Big[\big(x_j^{k+1} - m_k(x_i^k)\big) \big(\Phi_0(x_{j+}^{k+1}(x_i^k)) - \Phi_0(x_{j-}^{k+1}(x_i^k)) \big)$$
$$+ v_k(x_i^k) \big(\Phi_0'(x_{j+}^{k+1}(x_i^k)) - \Phi_0'(x_{j-}^{k+1}(x_i^k)) \big) \Big].$$

15

The diagonal terms of the Hessian matrix $\nabla^2 \widetilde{D}_{k+1}(\Gamma_{k+1})$ are given by:

$$
\frac{\partial^2 \widetilde{D}_{k+1}(\Gamma_{k+1})}{\partial^2 x_j^{k+1}} = \sum_{i=1}^{N_k} p_i^k \Big[\Phi_0(x_{j+}^{k+1}(x_i^k)) - \Phi_0(x_{j-}^{k+1}(x_i^k))
$$
$$
- \frac{1}{4v_k(x_i^k)} \Phi_0'(x_{j+}^{k+1}(x_i^k))(x_{j+1}^{k+1} - x_j^{k+1})
$$
$$
- \frac{1}{4v_k(x_i^k)} \Phi_0'(x_{j-}^{k+1}(x_i^k))(x_j^{k+1} - x_{j-1}^{k+1}) \Big]
$$

and its sub-diagonal terms are

$$
\frac{\partial^2 \widetilde{D}_{k+1}(\Gamma_{k+1})}{\partial x_j^{k+1} \partial x_{j-1}^{k+1}} = -\frac{1}{4} \sum_{i=1}^{N_k} p_i^k \frac{1}{v_k(x_i^k)} (x_j^{k+1} - x_{j-1}^{k+1}) \Phi_0'(x_{j-}^{k+1}(x_i^k)).
$$

The upper-diagonals terms are

$$
\frac{\partial^2 \widetilde{D}_{k+1}(\Gamma_{k+1})}{\partial x_j^{k+1} \partial x_{j+1}^{k+1}} = -\frac{1}{4} \sum_{i=1}^{N_k} p_i^k \frac{1}{v_k(x_i^k)} (x_{j+1}^{k+1} - x_j^{k+1}) \Phi_0'(x_{j+}^{k+1}(x_i^k)).
$$

A similar idea combining (vector or functional) optimal quantization with Newton-Raphson zero search procedure is used in [8] in a variance reduction context as an alternative and robust method to simulation based recursive importance sampling procedure to estimate the optimal change of measure. Furthermore, the convergence of the modified Newton-Raphson algorithm to the optimal quantizer is shown in the framework of [8] to be bounded by the quantization error. However, the tools used to show it do not apply directly in our context and the proof of the convergence of our modified Newton algorithm to an optimal quantizer remains an open question.

4.1.2 Computing the weights and the transition probabilities

Once we have access to the quadratic optimal quantizers Γ_k of the marginals $\widetilde{X}_k$, for $k = 0, \ldots, n$ (which are estimated using the Newton-Raphson algorithm described previously) we need to compute the associated weights $\mathbb{P}(\widetilde{X}_k \in C_j(\Gamma_k))$, $j = 1, \ldots, N_k$, for $k = 0, \ldots, n$ or the transition probabilities $\mathbb{P}(\widetilde{X}_k \in C_j(\Gamma_k)|\widetilde{X}_{k-1} \in C_i(\Gamma_{k-1}))$, $i = 1, \ldots, N_k$, $j = 1, \ldots, N_{k+1}$. We show in the next result how to compute them.

Proposition 4.1. *Let Γ_{k+1} be a quadratic optimal quantizer for the marginal random variable $\widetilde{X}_{k+1}$. Suppose that the quadratic optimal quantizer Γ_k for $\widetilde{X}_k$ and its companion weights $\mathbb{P}(\widetilde{X}_k \in C_i(\Gamma_k))$, $i = 1, \cdots, N_k$, are computed.*

1. The transition probability $p_{ij}^k = \mathbb{P}(\widetilde{X}_{k+1} \in C_j(\Gamma_{k+1})|\widetilde{X}_k \in C_i(\Gamma_k))$ is given by

$$
p_{ij}^k = p_i^k \Big(\Phi_0(x_{j+}^{k+1}(x_i^k)) - \Phi_0(x_{j-}^{k+1}(x_i^k)) \Big). \tag{38}
$$

2. The probability $p_j^{k+1} = \mathbb{P}(\widetilde{X}_{k+1} \in C_j(\Gamma_{k+1}))$ is given for every $j = 1, \cdots, N_{k+1}$ by

$$
p_j^{k+1} = \sum_{i=1}^{N_k} p_i^k \Big(\Phi_0(x_{j+}^{k+1}(x_i^k)) - \Phi_0(x_{j-}^{k+1}(x_i^k)) \Big). \tag{39}
$$

Proof. 1. For every $k \in \{1, \dots, n-1\}$, for every $i = 1, \dots, N_k$ and for every $j = 1, \dots, N_{k+1}$, we have

$$
\begin{aligned}
\mathbb{P}\big(\widetilde{X}_{k+1} \in C_j(\Gamma_{k+1}) | \widetilde{X}_k \in C_i(\Gamma_k)\big) &= \mathbb{P}\big(\widetilde{X}_{k+1} \in C_j(\Gamma_{k+1}) | \widehat{X}_k = x_i^{N_k}\big) \\
&= \mathbb{P}\big(\widetilde{X}_{k+1} \le x_{j+1/2}^{N_{k+1}} | \widehat{X}_k = x_i^{N_k}\big) - \mathbb{P}\big(\widetilde{X}_{k+1} \le x_{j-1/2}^{N_{k+1}} | \widehat{X}_k = x_i^{N_k}\big) \\
&= \Phi_0(x_{j+}^{k+1}(x_i^k)) - \Phi_0(x_{j-}^{k+1}(x_i^k)).
\end{aligned}
$$

2. We have for every $k \in \{1, \dots, n-1\}$ and for every $j = 1, \dots, N_{k+1}$,

$$
\begin{aligned}
\mathbb{P}\big(\widetilde{X}_{k+1} \in C_j(\Gamma_{k+1})\big) &= \mathbb{E}\big[\mathbb{P}\big(\widetilde{X}_{k+1} \in C_j(\Gamma_{k+1}) | \widehat{X}_k\big)\big] \\
&= \sum_{i=1}^{N_k} \mathbb{P}\big(\widetilde{X}_{k+1} \in C_j(\Gamma_{k+1}) | \widehat{X}_k = x_i^{N_k}\big) \mathbb{P}\big(\widetilde{X}_k \in C_i(\Gamma_k)\big).
\end{aligned}
$$

Now, il follows from the first assertion that

$$
\mathbb{P}\big(\widetilde{X}_{k+1} \in C_j(\Gamma_{k+1}) | \widehat{X}_k = x_i^{N_k}\big) = \Phi_0\big(x_{j+}^{k+1}(x_i^k)\big) - \Phi_0\big(x_{j-}^{k+1}(x_i^k)\big).
$$

This completes the proof. $\qquad\square$

5 Numerical examples

5.1 Numerical example for Brownian motion

We consider a real valued Brownian motion $(W_t)_{t \in [0,1]}$ and quantize the random variable W_1 by both regular marginal quantization and recursive marginal quantization methods. Denote by $D_M^{\mathrm{reg}}(\Gamma)$ the regular quantization distortion associated to W_1 and, for a given discretization mesh: $t_0 = 0 < \cdots < t_n = 1$ of size n, denote by $D_n^{\mathrm{rec}}(\Gamma_n)$ the distortion associated to the recursive quantization of W_1 at the end point $t_n = 1$.

We recall that for a given grid size M,

$$
D_M^{\mathrm{reg}}(\Gamma) = \mathbb{E}|W_1 - \widehat{W}_1^{\Gamma}|^2,
$$

where the optimal grid Γ for the regular marginal quantization is obtained by solving (using Newton-Raphson algorithm) the following minimization problem: $\inf_{\Gamma \in \mathbb{R}^M} D_M^{\mathrm{reg}}(\Gamma)$, which corresponds to the optimal grid of the standard Gaussian distribution. On the other hand,

$$
D_n^{\mathrm{rec}}(\Gamma_n) = \mathbb{E}|W_1 - \widehat{W}_1^{\Gamma_n}|^2,
$$

where Γ_n is the n-th component of the sequence of recursive marginal quantization grids $(\Gamma_k)_{k=0,\dots,n}$ defined for every $k = 0, \dots, n$ by

$$
\Gamma_k \in \mathrm{argmin}\{\widetilde{D}_k(\Gamma), \Gamma \subset \mathbb{R}, \mathrm{card}(\Gamma) \le N_k\},
$$

where

$$
\begin{aligned}
\widetilde{D}_k(\Gamma) := \mathbb{E}\big[\mathrm{dist}(\widetilde{W}_{t_k}, \Gamma)^2\big] &= \mathbb{E}\big[\mathrm{dist}\big(\widehat{W}_{t_{k-1}}^{\Gamma_{k-1}} + \sqrt{\Delta}Z_k, \Gamma\big)^2\big] \\
&= \sum_{i=1}^{N_{k-1}} \mathbb{E}\big[\mathrm{dist}\big(w_i^{k-1} + \sqrt{\Delta}Z_k, \Gamma\big)^2\big] \mathbb{P}\big(\widehat{W}_{t_{k-1}}^{\Gamma_{k-1}} = w_i^{k-1}\big)
\end{aligned}
$$

and $\widehat{W}_{t_{k-1}}^{\Gamma_{k-1}}$ is defined from the following recursion: $\widehat{W}_0^{\Gamma_0} = 0$ and for $\ell = 1, \ldots, k-1$,

$$\widetilde{W}_{t_\ell} = \widehat{W}_{t_{\ell-1}}^{\Gamma_{\ell-1}} + \sqrt{\Delta} Z_\ell \quad \text{and} \quad \widehat{W}_{t_\ell}^{\Gamma_\ell} = \mathrm{Proj}_{\Gamma_\ell}(\widetilde{W}_{t_\ell}), \ (Z_\ell)_{\ell=1,\ldots,k} \text{ is } i.i.d., \text{ and } \mathcal{N}(0;1)\text{-distributed.}$$

Our aim is precisely to compare the regular quantizations error $(D_M^{\mathrm{reg}}(\Gamma))^{1/2}$ and the recursive quantizations error $(\widetilde{D}_n^{\mathrm{rec}}(\Gamma_n))^{1/2}$ at time t_n of size N_n, for the same grid size $M = N_n$ (the choice of the grid size N_n depends on the used dispatching procedure and is specified further). To compute the quantity $D_n^{\mathrm{rec}}(\Gamma_n)$, we need to know the distribution of the couple of random variables $(W_1, \widehat{W}_1^{\Gamma_n})$ or $(W_1, \widetilde{W}_1)$, which distributions are unfortunately unknown.

This leads us to consider the following approximation for $D_n^{\mathrm{rec}}(\Gamma_n)$:

$$D_n^{\mathrm{rec}}(\Gamma_n) = \sum_{i=1}^{N_n} \mathbb{E}\left(|W_1 - w_i^n|^2 \mathbf{1}_{\{\widetilde{W}_1 \in C_i(\Gamma_n)\}}\right) \approx \widetilde{D}_n^{\mathrm{rec}}(\Gamma_n) := \sum_{i=1}^{N_n} \mathbb{E}\left(|W_1 - w_i^n|^2 \mathbf{1}_{\{W_1 \in C_i(\Gamma_n)\}}\right).$$

Therefore, we compare in practice the two quantities $(\widetilde{D}_n^{\mathrm{rec}}(\Gamma_n))^{1/2}$ and $(D_M^{\mathrm{reg}}(\Gamma))^{1/2}$. To this end, we fix first the mesh size $n = 50$ and we make the total budget $N = N_1 + \cdots + N_n$ (given that $N_0 = 1$) of the recursive grid sizes varying 50 by 50, from 250 up to 5000. We choose the sizes N_k following two procedures: the optimal and the uniform dispatching.

▷ *Uniform dispatching.* For a given global budget N, we make an "equal grid size dispatching" by choosing $N_k = N/n$, for $k = 1, \ldots, n$. If for example $N = N_1 + \cdots + N_n = 250$, we will have $N_k = 5$, for every $k \in \{1, \ldots, n\}$. For comparison tool with the regular quantization method we choose the size M of the regular quantization equal to N_n, for every fixed global budget N. The comparaison result is depicted on the right hand side graphic of Figure 1. In this figure, we plot the (approximated) recursive marginal quantization errors $(\widetilde{D}_n^{\mathrm{rec}}(\Gamma_n))^{1/2}$, for $|\Gamma_n| = 5, \ldots, 100$, and the regular quantization errors $(D_M^{\mathrm{reg}}(\Gamma))^{1/2}$, for $M = |\Gamma| = 5, \ldots, 100$.

▷ *Optimal dispatching.* In this case, the sizes N_k are obtained from the optimal dispatching procedure described in the PRACTIONNER CORNERS, (a). First of all, we have to choose the coefficients a_ℓ (appearing in Theorem 3.1) corresponding to the Brownian motion. Following, step by step, the proof of Theorem 3.1 and setting $\eta = 1$ (keep in mind that in the Brownian case $x_0 = 0$), we may improve our estimate for the coefficient a_ℓ. Namely, we have (at time $t_n = T$)

$$a_\ell = \left[\sqrt{\frac{2}{\pi}}(4 + \sqrt{\Delta})(e^{2t_\ell} - 1)\right]^{1/3}, \quad \ell = 1, \ldots, n.$$

Making N vary from 250 to 5000, the optimal dispatching leads to the following sizes for the grid Γ_n:

$$|\Gamma_n| \in \mathcal{G} = \{6, 8, 9, 10, 11, 13, \cdots, 123, 124, 126, 127\}.$$

Notice that we just display the first and the last ones values of $\mathcal{G}$ because it is of size 96. Here is how to read these values. If we fix the size of the global budget to $N = 250$, then the optimization procedure described in the PRACTIONNER CORNERS, (a), will generate the optimal grid sizes $N_1, N_2, \ldots, N_n$ inducing the minimal error bound in Theorem 3.1. In the set $\mathcal{G}$, we only display the size $N_n = N_{50}$ of the terminal grid Γ_{50} which then is equal to 6 for $N = 250$. So, to compare the regular quantization method and the recursive procedure with optimal dispatching and global budget $N = 250$, we have to put the grid size M of the regular quantization method to $M = 6$. If the global budget $N = 300$ then we choose $M = N_n = 8$, etc, and if $N = 5000$ then we choose $M = N_n = 127$.

The comparaison result is depicted on the left hand side of Figure 1. So, this figure plots the (approximated) recursive quantization errors $(\widetilde{D}_n^{\mathrm{rec}}(\Gamma_n))^{1/2}$, where $|\Gamma_n|$ is given by the optimal dispatching procedure, and the regular quantization errors $(D_M^{\mathrm{reg}}(\Gamma))^{1/2}$ for $M = |\Gamma_n| \in \mathcal{G}$.
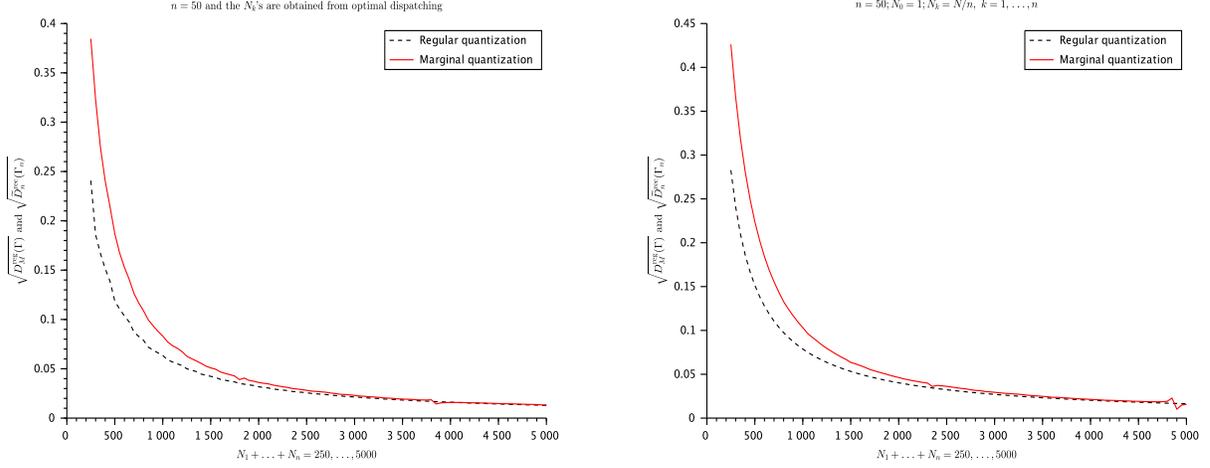
18

Figure 1: Comparison of the regular quantization (Regular quantization) of W_1 with its recursive marginal quantization (Marginal quantization) (where W is a Brownian motion). Abscissa axis: $n = 50$ and the total budget $N = N_1 + \cdots + N_n$ varies from 250 up to 5000. Ordinate axis: For a given N, (a) (left hand side graphic) we depict the recursive quantization errors $(\widetilde{D}_n^{\mathrm{rec}}(\Gamma_n))^{1/2}$ where $|\Gamma_n|$ is given by the optimal dispatching procedure, and the regular quantization errors $(D_M^{\mathrm{reg}}(\Gamma))^{1/2}$ for $M = |\Gamma_n|$; (b) (right hand side graphics) we set $N_k = N/n$, for $k = 1, \ldots, n$ and depict the recursive quantization errors $(\widetilde{D}_n^{\mathrm{rec}}(\Gamma_n))^{1/2}$, for $|\Gamma_n| = 5, \ldots, 100$, and the regular quantization errors $(D_M^{\mathrm{reg}}(\Gamma))^{1/2}$, for $M = |\Gamma| = 5, \ldots, 100$.
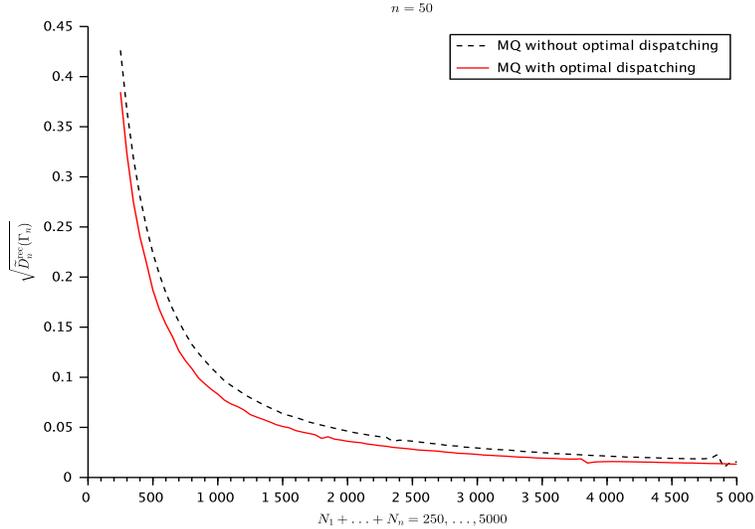
Figure 2: Comparison of the recursive marginal quantization errors. Abscissa axis: $n = 50$ and the total grid sizes $N = N_1 + \cdots + N_n$ varies from 250 up to 5000. Ordinate axis: on one hand, we set $N_k = N/n$, for $k = 1, \ldots, n$ and depict the (approximated) recursive quantization errors $(\widetilde{D}_n^{\mathrm{rec}}(\Gamma_n))^{1/2}$, for $|\Gamma_n| = 5, \ldots, 100$ (MQ without optimal dispatching), and, on the other hand, we depict the (approximated) recursive quantization errors $(\widetilde{D}_n^{\mathrm{rec}}(\Gamma_n))^{1/2}$ where $|\Gamma_n|$ is given by the optimal dispatching procedure (MQ with optimal dispatching).

19

Conclusion. The graphics of figure 1 and 2 suggest two observations. The first one is that, when the global budget N is too small, the regular quantization of W_1 is, as expected, more efficient than both recursive marginal quantizations (without and with optimal dispatching). But, when this global budget N increases, the absolute error between regular and recursive quantization methods fades and becomes close to zero up to 10^{-2}.

The second conclusion is that the recursive marginal quantization method with the optimal dispatching of the grid size over discretization time steps outperforms a setting where the grids are of equal sizes. However, when N increases, the recursive marginal quantization with optimal dispatching becomes, as expected, more time consuming while both methods yield almost the same results (the errors are equal up to 10^{-2}).

In the next section we propose an application of our method to the pricing of European options in a local volatility models. We remark that when using the marginal quantization methods, we have to choose a big global budget N to reach good price estimates. Like in the Brownian case, numerical results show that both recursive marginal quantization methods (with optimal and uniform dispatching) lead to the same price estimates (up to 10^{-3}) whereas the complexity of the optimal dispatching method becomes higher (as pointed out in the practitioner's corner). This is why we will use in the following section the recursive marginal quantization method with uniform dispatching procedure.

5.2 Pricing of European options in a local volatility model

5.2.1 The model

We consider a pseudo-CEV model (see e.g. [11]) where the dynamics of the stock price process is ruled by the following SDE (under the risk neutral probability)

$$dX_t = rX_t dt + \vartheta \frac{X_t^{\delta+1}}{\sqrt{1+X_t^2}} dW_t, \quad X_0 = x_0, \tag{40}$$

for some $\delta \in (0,1)$ and $\vartheta \in (0, \bar{\vartheta}]$ with $\bar{\vartheta} > 0$. The parameter r stands for the interest rate and $\sigma(x) := \vartheta \frac{x^\delta}{\sqrt{1+x^2}}$ corresponds to the local volatility function. This model becomes very close to the CEV model, specially when the initial value of the stock process X_0 is large enough. In this case the local volatility $\sigma(x) \approx \vartheta x^{\delta-1}$.

We aim at computing the price of a European Put option with payoff $(K - X_T)^+ = \max(K - X_T, 0)$, where K corresponds to the strike of the option and T to its maturity. Then we have to approximate the quantity

$$e^{-rT} \mathbb{E}(K - X_T)^+$$

where $\mathbb{E}$ stands for the expectation under the risk neutral probability. If the process $(\bar{X}_{t_k})_k$ denotes the discrete Euler process at regular time discretization steps t_k, with $0 = t_0 < \cdots < t_n = T$, associated to the diffusion process $(X_t)_{t \geq 0}$, this turns out to estimate

$$e^{-rT} \mathbb{E}(K - \bar{X}_T)^+$$

by optimal quantization. We estimate this quantity by the recursive marginal quantization method introduced in this paper and compare the numerical results with those obtained from standard Monte Carlo simulations.

20

	ϑ	MC (10^5)	RMQ ($N_k = 300$)	MC (10^6)	RMQ ($N_k = 400$)
	0.5	0.0022	0.0016	0.0018	0.0017
CI		[**0.0017**; **0.0028**]		[**0.0017**; **0.0019**]	
	0.6	0.0113	0.0108	0.0111	0.0110
CI		[**0.0101**; **0.0125**]		[**0.0107**; **0.0115**]	
	0.7	0.0377	0.0367	0.0373	0.0370
CI		[**0.0353**; **0.0401**]		[**0.0366**; **0.0381**]	
	0.8	0.0883	0.0867	0.0876	0.0871
CI		[**0.0843**; **0.0923**]		[**0.0863**; **0.0886**]	
	0.9	0.1696	0.1644	0.1659	0.1649
CI		[**0.1635**; **0.1756**]		[**0.1640**; **0.1678**]	
	1.0	0.267	0.270	0.271	0.271
CI		[**0.259**; **0.275**]		[**0.269**; **0.274**]	
	2.0	2.423	2.425	2.433	2.426
CI		[**2.387**; **2.459**]		[**2.422**; **2.445**]	
	3.0	5.424	5.475	5.492	5.478
CI		[**5.424**; **5.512**]		[**5.471**; **5.512**]	
	4.0	8.893	8.804	8.806	8.808
CI		[**8.801**; **8.986**]		[**8.777**; **8.835**]	

Table 1: (Pseudo-CEV model) Comparison of the Put prices obtained from Monte Carlo (MC) simulations (followed by its size) with associated confidence intervals (CI) and from the recursive marginal quantization (RMQ) method with equal grid size allocation $N_k = 300$ or $N_k = 400$, $\forall k = 1, \ldots, n$. The parameters are: $r = 0.15$; $\delta = 0.5$; $n = 120$; $T = 1$; $K = 100$; $X_0 = 100$; and for varying values of ϑ.

	K	MC (10^5)	MC (10^6)	RMQ ($N_k = 300$)	MC (10^7)	RMQ ($N_k = 400$)
	100	08.89	08.81	08.80	08.81	08.81
CI		[**08.80**; **08.99**]	[**08.78**; **08.84**]		[**08.80**; **08.82**]	
	105	10.61	10.60	10.59	10.59	10.59
CI		[**10.51**; **10.72**]	[**10.57**; **10.63**]		[**10.58**; **10.60**]	
	110	12.53	12.57	12.57	12.57	12.57
CI		[**12.42**; **12.64**]	[**12.53**; **12.60**]		[**12.56**; **12.58**]	
	115	14.72	14.74	14.75	14.75	14.75
CI		[**14.60**; **14.84**]	[**14.70**; **14.78**]		[**14.75**; **14.77**]	
	120	17.18	17.10	17.11	17.13	17.12
CI		[**17.04**; **17.31**]	[**17.06**; **17.15**]		[**17.11**; **17.14**]	
	125	19.64	19.69	19.66	19.67	19.67
CI		[**19.50**; **19.78**]	[**19.64**; **19.73**]		[**19.65**; **19.68**]	
	130	22.41	22.32	22.39	22.40	22.40
CI		[**22.26**; **22.56**]	[**22.32**; **22.41**]		[**22.38**; **22.41**]	

Table 2: (Pseudo-CEV model) Comparison of the Put prices obtained from Monte Carlo (MC) simulations (followed by its size) with associated confidence intervals (CI) and from the recursive marginal quantization (RMQ) method method with equal grid size allocation $N_k = 300$ or $N_k = 400$, $\forall k = 1, \ldots, n$. The parameters are: $r = 0.15$; $n = 120$; $N_k = 400$, $\forall k = 1, \ldots, n$; $T = 1$; $\vartheta = 4$; $X_0 = 100$; and for varying values of K.

5.2.2 Numerical results

To deal with numerical examples we set $\delta = 0.5$, $X_0 = 100$, and choose the interest rate $r = 0.15$. We discretize the price process using the Euler scheme with $n = 120$ (regular) discretization steps and quantize the Euler marginal processes by our proposed method. For $k = 1, \ldots, n$, we put all the marginal quantization grid sizes N_k equal to 300 and then, to 400 (recall that $\widehat{X}_0 = X_0 = 100$ and $N_0 = 1$). We estimate the price of the Put option by

$$\mathbb{E}\big[\big(K - \widehat{X}_{t_n}^{\Gamma_n}\big)^+\big] = \sum_{i=1}^{N_n}(K - x_i^{N_n})^+ \, \mathbb{P}\big(\widehat{X}_{t_n}^{\Gamma_n} = x_i^{N_n}\big) \tag{41}$$

where $t_n = T$, and where $\Gamma_n = \{x_1^{N_n}, \cdots, x_{N_n}^{N_n}\}$ is the quantizer of size N_n computed from the Newton-Raphson algorithm (with 5 iterations) and where the associated weight are estimated from (39).

We compare the prices obtained from the recursive marginal quantization (RMQ) method with those obtained by the Monte Carlo (MC) simulations for various values of ϑ with a fixed strike $K = 100$ (see Table 1) or for varying values of the strike K with a fixed $\vartheta = 4$ (see Table 2). For the Monte Carlo simulations we set the sample size M_{mc} equal to 10^5 and 10^6 for $K = 100$ and to $M_{\mathrm{mc}} = 10^5$, 10^6 and 10^7 when making the strike K varying.

Remark 5.1. (*on the computation time*) (a) Remark that all the quantization grids Γ_k of sizes $N_k = 300$ (and $N_k = 400$), for every $k = 1, \ldots, n = 120$, and there companion weights are obtained in around 40 seconds (and 1 minute) from the Newton-Raphson algorithm with 5 iterations. Computations are performed using *Scilab* software on a CPU 2.7 GHz and 4 Go memory computer.

(b) It is clear that once the grids and the associated weights are available, the estimation of the price by RMQ method using the sum (41) is instantaneous.

Remark 5.2. (*Initialization of the Newton-Raphson algorithm*) Let $0 = t_0 < \cdots < t_n$ be the time discretization steps, let $X_0 = x$ be the present value of the stock price process and suppose that the grid sizes N_k are all equal. Since the random variable $\bar{X}_{t_1} \sim \mathcal{N}(m_0(x); v_0^2(x))$, in order to compute the (optimal) N_1-quantizer for $\bar{X}_{t_1}$ we initialize the algorithm to $v_0(x)z^{N_1} + m_0(x)$, where z^{N_1} is the optimal N_1-quantizer of the $\mathcal{N}(0; 1)$. Once we get the optimal N_1-quantization Γ_1 for $\bar{X}_{t_1}$ and its companion weights, we initialize the algorithm to Γ_1 to perform the optimal N_2-quantizer for $\bar{X}_{t_2}$ and its companion weights, $\cdots$, and so on, until we get the optimal N_n-quantizer for $\bar{X}_{t_n}$ and the associated weights. Notice that doing so we observe no failure of the convergence in all the considered examples.

Remark 5.3. We show in Figure 3 and Figure 4 two graphics where we depict on the abscissa axis the optimal grids (of sizes $N_k = 150$) and on the ordinate axis the corresponding weights. The dynamics of the price process in Figure 3 is given by

$$dX_t = rX_t dt + \sigma X_t dW_t, \quad X_0 = 86.3$$

with $r = 0.03$, $\sigma = 0.05$ whereas its dynamics in Figure 4 is given by

$$dX_t = rX_t dt + \vartheta \frac{X_t^{\delta+1}}{\sqrt{1 + X_t^2}} dW_t, \quad X_0 = 100$$

with $r = 0.15$, $\vartheta = 0.7$, $\delta = 0.5$.

For our numerical examples, we remark first that in all examples the prices obtained by RMQ (of sizes $N_k = 300$ and $N_k = 400$, $\forall k = 1, \cdots, n$) stay in the confidence interval induced by the MC price estimates. On the other hand the prices obtained by the RMQ (of sizes $N_k = 400$) method are

more precise (more especially when $\vartheta = 4$ and K grows away from 100) than those obtained by the MC method when $M_{\mathrm{mc}} = 10^5$ or 10^6. Consequently, the RMQ method seems to be more efficient than the MC when the sample size is less than 10^6. However, when increasing the sample size to $M_{\mathrm{mc}} = 10^7$ the two prices become closer (up to 10^{-2}). We also remark that, up to 10^{-2}, the prices obtained from RMQ of both different sizes ($N_k = 300$ and $N_k = 400$) are equal.

Remark 5.4. We remark that when the Monte Carlo sample size $M_{\mathrm{mc}} = 10^6$ (resp. $M_{\mathrm{mc}} = 10^7$) it takes about 1 minute and 40 seconds (resp. 2 minutes and 30 seconds) to get a price using the *C programming language* on the same computer described previously. Then, in this situation, it takes much more time to obtain a price by MC method than by RMQ for a fixed precision in the price approximations.

To strengthen the previous conclusions related to the local volatility model we compare the two methods in the Black-Scholes framework where the stock price process evolves following the dynamics:

$$dX_t = rX_t dt + \sigma X_t dW_t, \quad X_0 = 100.$$

In this setting the true prices are available and will serve us as a support for comparisons. The parameters are chosen so that the model remains close to the Pseudo-CEV model: $r = 0.15$ and $\sigma \approx \vartheta X_0^{\delta-1}$. Numerical results are printed in Tables 3 and Table 4 and confirm our conclusions on the Pseudo-CEV model. We notice that in the Black-Scholes model, the estimated prices from the RMQ (for both size choice) method are close to the true prices (the best absolute error is of order 10^{-5} for a volatility $\sigma = 5\%$ and the worse absolute error 2.10^{-2} is achieved with high volatility: $\sigma = 40\%$). This shows the robustness of the RMQ method even for reasonably high values of the volatility.

σ	MC (10^5)	RMQ ($N_k = 300$)	MC (10^6)	RMQ ($N_k = 400$)	True price
0.05	0.0015 [0.0012; 0.0019]	0.00178 1.10^{-5}	0.00178 [0.0017; 0.0019]	0.00176 1.10^{-5}	0.00177
0.06	0.0116 [0.0104; 0.0128]	0.0108 4.10^{-4}	0.0109 [0.0106; 0.0113]	0.0109 3.10^{-4}	0.0112
0.07	0.0365 [0.0342; 0.0387]	0.0366 7.10^{-4}	0.0370 [0.0363; 0.0378]	0.0369 4.10^{-4}	0.0373
0.08	0.0876 [0.0836; 0.0915]	0.0865 1.10^{-3}	0.0876 [0.0863; 0.0888]	0.0869 6.10^{-4}	0.0875
0.09	0.1666 [0.1607; 0.1724]	0.1641 1.10^{-3}	0.1644 [0.1622; 0.1658]	0.1647 7.10^{-4}	0.1654
0.10	0.269 [0.261; 0.277]	0.270 2.10^{-3}	0.271 [0.271; 0.273]	0.271 1.10^{-3}	0.272
0.20	2.444 [2.410; 2.479]	2.422 5.10^{-3}	2.431 [2.420; 2.442]	2.424 3.10^{-3}	2.427
0.30	5.455 [5.395; 5.515]	5.466 8.10^{-3}	5.469 [5.450; 5.549]	5.470 4.10^{-3}	5.474
0.40	8.680 [8.598; 8.763]	8.785 7.10^{-3}	8.787 [8.760; 8.813]	8.790 2.10^{-3}	8.792

Table 3: (Black-Scholes model) Comparison of the Put prices obtained from Monte Carlo (MC) simulations (followed by its size) with associated confidence intervals and from marginal quantization (RMQ) method with equal grid size allocation $N_k = 300$ or $N_k = 400$, $\forall k = 1, \ldots, n$, with the associated absolute error (under each displayed RMQ price) w. r. t. the true price. The parameters are: $n = 120$; $T = 1$; $r = 0.15$; $K = 100$; $X_0 = 100$ for varying values of σ.

K	MC (10^5)	RMQ ($N_k = 300$)	MC (10^6)	RMQ ($N_k = 400$)	True price
100	8.680	8.785	8.787	8.790	8.792
	$[\mathbf{8.598; 8.763}]$	$\mathbf{7.10^{-3}}$	$[\mathbf{8.760; 8.813}]$	$\mathbf{2.10^{-3}}$	
105	10.805	10.740	10.739	10.744	10.750
	$[\mathbf{10.71; 10.90}]$	$\mathbf{1.10^{-2}}$	$[\mathbf{10.71; 10.90}]$	$\mathbf{6.10^{-3}}$	
110	12.86	12.90	12.89	12.90	12.91
	$[\mathbf{12.76; 12.96}]$	$\mathbf{1.10^{-2}}$	$[\mathbf{12.86; 12.93}]$	$\mathbf{1.10^{-2}}$	
115	15.29	15.25	15.24	15.26	15.27
	$[\mathbf{15.18; 15.40}]$	$\mathbf{1.10^{-2}}$	$[\mathbf{15.21; 15.28}]$	$\mathbf{1.10^{-2}}$	
120	17.66	17.80	17.81	17.79	17.81
	$[\mathbf{17.54; 17.79}]$	$\mathbf{1.10^{-2}}$	$[\mathbf{17.78; 17.85}]$	$\mathbf{1.10^{-2}}$	
125	20.56	20.50	20.50	20.50	20.52
	$[\mathbf{20.43; 20.69}]$	$\mathbf{2.10^{-2}}$	$[\mathbf{20.46; 20.54}]$	$\mathbf{1.10^{-2}}$	
130	23.28	23.37	23.37	23.37	23.39
	$[\mathbf{23.14; 23.42}]$	$\mathbf{2.10^{-2}}$	$[\mathbf{23.34; 23.43}]$	$\mathbf{2.10^{-2}}$	

Table 4: (Black-Scholes model) Comparison of the Put prices obtained from Monte Carlo (MC) simulations (followed by the size of the MC between brackets) with associated confidence intervals and from the marginal quantization (RMQ) method with equal grid size allocation $N_k = 300$ or $N_k = 400$, $\forall k = 1, \ldots, n$, with the associated absolute error (under each displayed RMQ price) w. r. t. the true price. The parameters are: $n = 120$; $T = 1$; $r = 0.15$; $\sigma = 40\%$; $X_0 = 100$ for varying values of K.
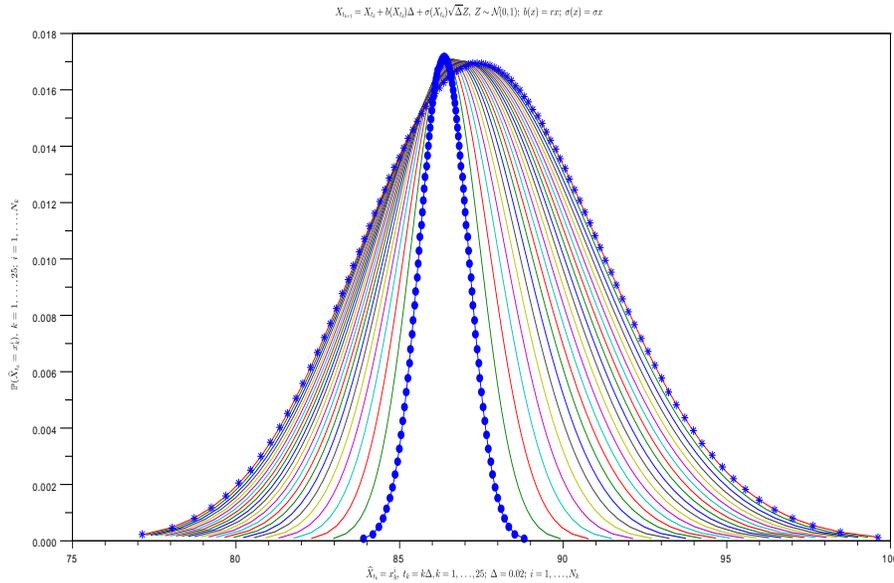

Figure 3: ("Black-Scholes model ") $dX_t = rX_t dt + \sigma X_t dW_t$, $X_0 = 86.3$, $r = 0.03$, $\sigma = 0.05$. Abscissa axis: the optimal grids, $\widehat{X}_{t_k} = x_k^i$, $t_k = k\Delta$, $\Delta = 0.02$, $k = 1, \ldots, 25$, $i = 1, \ldots, N_k$. Ordinate axis: the associated weights, $\mathbb{P}(\widehat{X}_{t_k} = x_k^i)$, $k = 1, \ldots, 25$, $i = 1, \ldots, N_k$. $\widehat{X}_{t_1}$ is depicted in dots '•', $\widehat{X}_{t_{25}}$ is represented by the symbol '*', $t_1 = 0.02$ and $t_{25} = 0.5$ and the remaining in continuous line
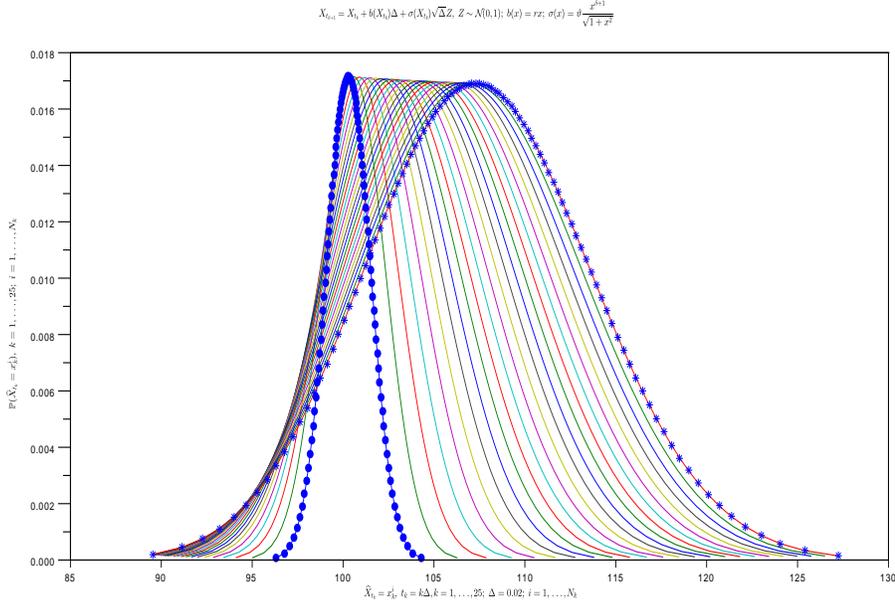
$$X_{t_{k+1}} = X_{t_k} + b(X_{t_k})\Delta + \sigma(X_{t_k})\sqrt{\Delta}Z, \ Z \sim \mathcal{N}(0,1); \ b(x) = rx; \ \sigma(x) = \vartheta \frac{x^{\delta+1}}{\sqrt{1+x^2}}$$

Figure 4: ("Pseudo-CEV model") $dX_t = rX_t dt + \vartheta(X_t^{\delta+1}/(1+X_t^2)^{-1/2})dW_t$, $X_0 = 100$, $r = 0.15$, $\vartheta = 0.7$, $\delta = 0.5$. Abscissa axis: the optimal grids, $\widehat{X}_{t_k} = x_k^i$, $t_k = k\Delta$, $\Delta = 0.02$, $k = 1, \ldots, 25$, $i = 1, \ldots, N_k$. Ordinate axis: the associated weights. $\widehat{X}_{t_1}$ is depicted in dots '•', $\widehat{X}_{t_{25}}$ is represented by the symbol '*', $t_1 = 0.02$ and $t_{25} = 0.5$ and the remaining in continuous line.

Appendix

The proof of Lemma 3.2 needs an additional result given below as a technical Lemma.

Lemma. Let $a \in \mathbb{R}^d$ et let $p \in [2, 3]$. Then,

$$\forall u \in \mathbb{R}^d, \quad |a + u|^p \le |a|^p + p|a|^{p-2}(a|u) + \frac{p(p-1)}{2}\left(|a|^{p-2}|u|^2 + |u|^p\right). \tag{42}$$

Proof. Define the function $g(u) = |a + u|^p$, $u \in \mathbb{R}^d$. We have (denoting by $u^\star$ the transpose of the the column vector $u \in \mathbb{R}^d$),

$$\nabla g(u) = p|a+u|^{p-1}\frac{a+u}{|a+u|} \quad \text{and} \quad \nabla^2 g(u) = p(p-2)|a+u|^{p-2}\frac{(a+u)(a+u)^\star}{|a+u|^2} + p|a+u|^{p-2}I_d.$$

where I_d is the identity on $\mathbb{R}^d$. It follows from the Taylor-Lagrange formula that

$$|a+u|^p = |a|^p + p|a|^{p-2}(a|u) + \frac{p(p-2)}{2}|a+\xi|^{p-2}\frac{(a+\xi|u)^2}{|a+\xi|^2} + \frac{p}{2}|a+\xi|^{p-2}|u|^2,$$

where $(\cdot|\cdot)$ stands for the inner product and $\xi = \lambda_u u$, $\lambda_u \in [0, 1]$. Moreover $\frac{(a+\xi|u)^2}{|a+\xi|^2} \le |u|^2$ owing to Cauchy-Schwarz inequality. Hence

$$|a+u|^p \le |a|^p + p|a|^{p-2}(a|u) + \frac{p(p-2)}{2}|a+\xi|^{p-2}|u|^2 + \frac{p}{2}|a+\xi|^{p-2}|u|^2$$

$$\le |a|^p + p|a|^{p-2}(a|u) + \frac{p(p-1)}{2}|a+\xi|^{p-2}|u|^2.$$

Then, the result follows since $|a + \xi|^{p-2} \le |a|^{p-2} + |u|^{p-2}$ since $p - 2 \in [0, 1]$) and $|\xi| \le |u|$. $\qquad\square$

We are now in position to prove Proposition 3.2.

Proof. *(of Lemma 3.2.)* The proof will be split into three steps.

STEP 1. Let A be a $d \times q$-matrix. We prove that for any random variable Z such that $\mathbb{E}(Z) = 0$ and $Z \in L^p(\Omega, \mathcal{A}, \mathbb{P})$

$$\mathbb{E}|a + \sqrt{\Delta}AZ|^p \le \Big(1 + \frac{(p-1)(p-2)}{2}\Delta\Big)|a|^p + \Delta\Big(1 + p + \Delta^{\frac{p}{2}-1}\Big)\|A\|^p\mathbb{E}|Z|^p,$$

where $\|A\|^2 = \mathrm{Tr}(AA^\star)$. In fact, it follows from Equation (42) that

$$|a + \sqrt{\Delta}AZ|^p \le |a|^p + p\Delta^{\frac{1}{2}}|a|^{p-2}(a|AZ) + \frac{p(p-1)}{2}\Big(|a|^{p-2}\Delta|AZ|^2 + \Delta^{\frac{p}{2}}|AZ|^p\Big).$$

Applying Young's inequality with conjugate exponents $p' = \frac{p}{p-2}$ and $q' = \frac{p}{2}$, we get

$$|a|^{p-2}\Delta|AZ|^2 \le \Delta\Big(\frac{|a|^p}{p'} + \frac{|AZ|^p}{q'}\Big),$$

which leads to

$$|a + \sqrt{\Delta}AZ|^p \le |a|^p + p\Delta^{\frac{1}{2}}|a|^{p-2}(a|AZ) + \frac{p(p-1)}{2}\Big(\frac{\Delta}{p'}|a|^p + \Big(\frac{\Delta}{q'} + \Delta^{\frac{p}{2}}\Big)|AZ|^p\Big)$$

$$\le |a|^p\Big(1 + \frac{p(p-1)}{2p'}\Delta\Big) + p\Delta^{\frac{1}{2}}|a|^{p-2}(a|AZ) + \Delta\Big(\frac{p(p-1)}{2q'} + \Delta^{\frac{p}{2}-1}\Big)|AZ|^p.$$

Taking the expectation yields (owing to the fact that $\mathbb{E}(Z) = 0$)

$$\mathbb{E}|a + \sqrt{\Delta}AZ|^p \le \Big(1 + \frac{(p-1)(p-2)}{2}\Delta\Big)|a|^p + \Delta\Big(1 + p + \Delta^{\frac{p}{2}-1}\Big)\mathbb{E}|AZ|^p.$$

As a consequence, we get

$$\mathbb{E}|a + \sqrt{\Delta}AZ|^p \le \Big(1 + \frac{(p-1)(p-2)}{2}\Delta\Big)|a|^p + \Delta\Big(1 + p + \Delta^{\frac{p}{2}-1}\Big)\|A\|^p\mathbb{E}|Z|^p.$$

STEP 2. Keeping in mind the result of the first step and setting for every $t \in [0, T]$ and $x \in \mathbb{R}^d$, $a := x + \Delta b(t, x)$ and $A := \sigma(t, x)$, we get (owing to the linear growth assumption on the coefficients of the diffusion process)

$$|a| \le |x|(1 + L\Delta) + L\Delta \quad \text{and} \quad \|A\|^p \le L_p(1 + |x|^p),$$

where $L_p = 2^{p-1}L^p$. It follows that (keep in mind that $p \in (2, 3]$)

$$\begin{aligned}
|a|^p &\le (1 + 2L\Delta)^p\Big(\frac{1 + L\Delta}{1 + 2L\Delta}|x| + \frac{L\Delta}{1 + 2L\Delta}\Big)^p \\
&\le (1 + 2L\Delta)^p\Big(\frac{1 + L\Delta}{1 + 2L\Delta}|x|^p + \frac{L\Delta}{1 + 2L\Delta}\Big) \\
&\le (1 + 2L\Delta)^p|x|^p + (1 + 2L\Delta)^{p-1}L\Delta.
\end{aligned}$$

Then, we derive

$$\begin{aligned}
\mathbb{E}|a + \sqrt{\Delta}AZ|^p \le{}& \Big(1 + \frac{(p-1)(p-2)}{2}\Delta\Big)(1 + 2L\Delta)^p|x|^p \\
&+ \Big(1 + \frac{(p-1)(p-2)}{2}\Delta\Big)(1 + 2L\Delta)^{p-1}L\Delta \\
&+ \Delta L_p\Big(1 + p + \Delta^{\frac{p}{2}-1}\Big)(1 + |x|^p)\,\mathbb{E}|Z|^p.
\end{aligned}$$

Using the inequality $1 + u \leq e^u$, for every $u \in \mathbb{R}$, we finally get

$$\mathbb{E}|a + \sqrt{\Delta}AZ|^p \leq \left(e^{\kappa_p \Delta} + K_p \Delta\right)|x|^p + \left(e^{\kappa_p \Delta}L + K_p\right)\Delta,$$

where $\kappa_p := \left(\frac{(p-1)(p-2)}{2} + 2pL\right)$ and $K_p := L_p\left(1 + p + \Delta^{\frac{p}{2}-1}\right)\mathbb{E}|Z|^p$.

STEP 3. Now, owing to the previous step and to the fact that for every $k = 1, \ldots, n$, Z_k is independent from $\widehat{X}_{k-1}$, we have

$$\begin{aligned}
\mathbb{E}|\widetilde{X}_k|^p &= \mathbb{E}\big[\mathbb{E}(|\mathcal{E}_k(\widehat{X}_{k-1}, Z_k)|^p|\widehat{X}_{k-1})\big] \\
&\leq \left(e^{\kappa_p \Delta} + K_p \Delta\right)\mathbb{E}|\widehat{X}_{k-1}|^p + \left(e^{\kappa_p \Delta}L + K_p\right)\Delta.
\end{aligned}$$

Since by construction, $\widehat{X}_k$ is a stationary quantizer (with respect to $\widetilde{X}_k$) for every $k = 0, \ldots, n$, we get

$$\begin{aligned}
\mathbb{E}|\widetilde{X}_k|^p &= \left(e^{\kappa_p \Delta} + K_p \Delta\right)\mathbb{E}\big|\mathbb{E}(\widetilde{X}_{k-1}|\widehat{X}_{k-1})\big|^p + \left(e^{\kappa_p \Delta}L + K_p\right)\Delta \\
&\leq \left(e^{\kappa_p \Delta} + K_p \Delta\right)\mathbb{E}\big(\mathbb{E}(|\widetilde{X}_{k-1}|^p|\widehat{X}_{k-1})\big) + \left(e^{\kappa_p \Delta}L + K_p\right)\Delta \qquad \text{(Jensen's inequality)} \\
&= \left(e^{\kappa_p \Delta} + K_p \Delta\right)\mathbb{E}|\widetilde{X}_{k-1}|^p + \left(e^{\kappa_p \Delta}L + K_p\right)\Delta.
\end{aligned}$$

We show by induction that for every $k = 1, \ldots, n$,

$$\begin{aligned}
\mathbb{E}|\widetilde{X}_k|^p &\leq \left(e^{\kappa_p \Delta} + K_p \Delta\right)^k \mathbb{E}|\widetilde{X}_0|^p + \left(e^{\kappa_p \Delta}L + K_p\right)\Delta \sum_{j=0}^{k-1}\left(e^{\kappa_p \Delta} + K_p \Delta\right)^j \\
&\leq e^{\kappa_p k \Delta}\left(1 + K_p \Delta e^{-\kappa_p \Delta}\right)^k|x_0|^p + \left(e^{\kappa_p \Delta}L + K_p\right)\Delta \sum_{j=0}^{k-1}e^{\kappa_p j \Delta}\left(1 + K_p \Delta e^{-\kappa_p \Delta}\right)^j.
\end{aligned}$$

Using the inequality $1 + u \leq e^u$, for every $u \in \mathbb{R}$, yields

$$\begin{aligned}
\mathbb{E}|\widetilde{X}_k|^p &\leq e^{\kappa_p k \Delta}\left(1 + K_p \Delta\right)^k|x_0|^p + \left(e^{\kappa_p \Delta}L + K_p\right)\Delta \sum_{j=0}^{k-1}e^{\kappa_p j \Delta}\left(1 + K_p \Delta\right)^j \\
&\leq e^{(\kappa_p + K_p)k \Delta}|x_0|^p + \left(e^{\kappa_p \Delta}L + K_p\right)\Delta \sum_{j=0}^{k-1}e^{(\kappa_p + K_p)j \Delta} \\
&= e^{(\kappa_p + K_p)t_k}|x_0|^p + \Delta\left(e^{\kappa_p \Delta}L + K_p\right)\frac{e^{(\kappa_p + K_p)t_k} - 1}{e^{(\kappa_p + K_p)\Delta} - 1} \\
&\leq e^{(\kappa_p + K_p)t_k}|x_0|^p + \left(e^{\kappa_p \Delta}L + K_p\right)\frac{e^{(\kappa_p + K_p)t_k} - 1}{\kappa_p + K_p}.
\end{aligned}$$

The last inequality follows from the fact that $e^{(\kappa_p + K_p)\Delta} - 1 \geq (\kappa_p + K_p)\Delta$. $\qquad\square$

References

[1] V. Bally and G. Pagès. A quantization algorithm for solving discrete time multidimensional optimal stopping problems, Bernoulli, 9(6), 1003-1049, 2003.

[2] V. Bally, G. Pagès and J. Printems. A quantization tree method for pricing and hedging multidimensional American options. *Mathematical Finance*, 15(1), 119-168, 2005.

[3] V. Bally and D. Talay. The law of the Euler scheme for stochastic differential equations (II): convergence rate of the density. *Monte Carlo Methods and Applications*, 2, 93-128, 1996.

[4] O. Bardou, S. Bouthemy and G. Pagès. Optimal quantization for pricing of swing options. *Applied Mathematical Finance*, 16(2), 183-217, 2009.

[5] J. A. Bucklew and G. L. Wise. Multidimensional asymptotic quantization theory with r-th power distribution measures. *IEEE Trans. Inform. Theory*, 28, 239-247, 1982.

[6] G. Callegaro, A. Sagna. An application to credit risk of a hybrid Monte Carlo-optimal quantization method. *The Journal of Computational Finance*, 16, 123-156, 2013.

[7] M. Corsi, H. Pham and W. Runggaldier. Numerical approximation by quantization of control problems in finance under partial observations. *Mathematical modeling and numerical methods in finance, special volume of Handbook of Numerical analysis*, 2009.

[8] N. Frikha and A. Sagna. Quantization based recursive Importance Sampling. *Monte Carlo Methods and Applications*, 18, 287-326, 2012.

[9] A. Gersho and R. Gray. *Vector Quantization and Signal Compression*. Kluwer Academic Press, Boston, 1992.

[10] S. Graf and H. Luschgy. *Foundations of Quantization for Probability Distributions*. Lect. Notes in Math., 1730, 2000. Berlin: Springer.

[11] V. Lemaire and G. Pagès. Unconstrained Recursive Importance Sampling. *Annals of Applied Probability*, 20, 1029-1067, 2010.

[12] H. Luschgy and G. Pagès. Functional quantization and mean regularity of processes with an application to Lévy processes. *The Annals of Applied Probability*, 18(2), 427-469, 2008.

[13] G. Pagès. Introduction to optimal vector quantization and its applications to numerics. *ESAIM Proc. & Survey*, 48, 29-79, 2015.

[14] G. Pagès. A space quantization method for numerical integration. *Journal of Computational and Applied Mathematics*, 89, 1-38, 1998.

[15] G. Pagès and H. Pham. Optimal quantization methods for nonlinear filtering with discrete time observations. *Bernoulli*, 11(5), 893-932, 2005.

[16] G. Pagès, H. Pham and J. Printems. An Optimal markovian quantization algorithm for multidimensional stochastic control problems. *Stochastics and Dynamics*, 4(4), 501-545, 2004.

[17] G. Pagès and J. Printems. Optimal quadratic quantization for numerics: the gaussian case. *Monte Carlo Methods and Applications*, 9(2), 135-165, 2003.

[18] G. Pagès and J. Printems. Functional quantization for numerics with an application to option pricing. *Monte Carlo Methods and Applications*, 11(4), 407-446, 2005.

[19] G. Pagès and A. Sagna. Asymptotics of the maximal radius of an L^r-optimal sequence of quantizers. *Bernoulli*, 18(1), 360-389, 2012.

[20] G. Pagès and A. Sagna. Componentwise product quantization of an $\mathbb{R}^d$-valued Euler diffusion process with applications. *In preparation*.

[21] G. Pagès and J. Yu. Pointwise convergence of the Lloyd algorithm in higher dimension. *Preprint LPMA*.

[22] H. Pham, W. Runggaldier and A. Sellami. Approximation by quantization of the filter process and applications to optimal stopping problems under partial observation. *Monte Carlo Methods and Applications*, 11, 57-82, 2005.

[23] C. Profeta and A. Sagna. Conditional hitting time estimation in a nonlinear filtering model by the Brownian bridge method. Preprint. Submitted work.

[24] A. Sagna. Pricing of barrier options by marginal functional quantization method. *Monte Carlo Methods and Applications*, 17(4), 371-398, 2012.

[25] W. F. Sheppard. On the Calculation of the Most Probable Values of Frequency-Constants, for Data Arranged According to Equidistant Divisions of Scale, Proc. London Math. Soc. 29, 353-380, 1898.

[26] D. Talay and L. Tubaro. Expansion of the global error for numerical schemes solving stochastic differential equations. *Stochastic Analysis and Applications*, 8(4), 94-120, 1990.

[27] R. Usmani, Inversion of a tridiagonal Jacobi matrix. *Linear Algebra Appl.*, 212/213, 413-414, 1994.

[28] P. Zador. Asymptotic quantization error of continuous signals and the quantization dimension. *IEEE Trans. Inform. Theory*, 28, 139-149, 1982.